

9-27-2023

SynLight: A Bicistronic Strategy for Simultaneous Active Zone and Cell Labeling in the *Drosophila* Nervous System

Michael A. Aimino

Jesse Humenik

Michael J. Parisi

Juan Carlos Duhart

Timothy J. Mosca

Follow this and additional works at: <https://jdc.jefferson.edu/farberneursofp>




Part of the [Nervous System Commons](#), and the [Neurosciences Commons](#)

[Let us know how access to this document benefits you](#)

This Article is brought to you for free and open access by the Jefferson Digital Commons. The Jefferson Digital Commons is a service of Thomas Jefferson University's [Center for Teaching and Learning \(CTL\)](#). The Commons is a showcase for Jefferson books and journals, peer-reviewed scholarly publications, unique historical collections from the University archives, and teaching tools. The Jefferson Digital Commons allows researchers and interested readers anywhere in the world to learn about and keep up to date with Jefferson scholarship. This article has been accepted for inclusion in Farber Institute for Neuroscience Faculty Papers by an authorized administrator of the Jefferson Digital Commons. For more information, please contact: JeffersonDigitalCommons@jefferson.edu.

SynLight: a bicistronic strategy for simultaneous active zone and cell labeling in the *Drosophila* nervous system

Michael A. Aimino, Jesse Humenik, Michael J. Parisi, Juan Carlos Duhart, Timothy J. Mosca *

Department of Neuroscience, Vickie and Jack Farber Institute of Neuroscience, Thomas Jefferson University, Bluemle Life Sciences Building, Philadelphia, PA 19107, USA

*Corresponding author: Department of Neuroscience, Vickie and Jack Farber Institute of Neuroscience, Thomas Jefferson University, Bluemle Life Sciences Building, Philadelphia, PA 19107, USA. Email: timothy.mosca@jefferson.edu

At synapses, chemical neurotransmission mediates the exchange of information between neurons, leading to complex movement, behaviors, and stimulus processing. The immense number and variety of neurons within the nervous system make discerning individual neuron populations difficult, necessitating the development of advanced neuronal labeling techniques. In *Drosophila*, Bruchpilot-Short and mCD8-GFP, which label presynaptic active zones and neuronal membranes, respectively, have been widely used to study synapse development and organization. This labeling is often achieved via the expression of 2 independent constructs by a single binary expression system, but expression can weaken when multiple transgenes are expressed by a single driver. Recent work has sought to circumvent these drawbacks by developing methods that encode multiple proteins from a single transcript. Self-cleaving peptides, specifically 2A peptides, have emerged as effective sequences for accomplishing this task. We leveraged 2A ribosomal skipping peptides to engineer a construct that produces both Bruchpilot-Short-mStraw and mCD8-GFP from the same mRNA, which we named SynLight. Using SynLight, we visualized the putative synaptic active zones and membranes of multiple classes of olfactory, visual, and motor neurons and observed the correct separation of signal, confirming that both proteins are being generated separately. Furthermore, we demonstrate proof of principle by quantifying synaptic puncta number and neurite volume in olfactory neurons and finding no difference between the synapse densities of neurons expressing SynLight or neurons expressing both transgenes separately. At the neuromuscular junction, we determined that the synaptic puncta number labeled by SynLight was comparable to the endogenous puncta labeled by antibody staining. Overall, SynLight is a versatile tool for examining synapse density in any nervous system region of interest and allows new questions to be answered about synaptic development and organization.

Keywords: synapse; 2A peptides; fluorescent labeling; antennal lobe; optic lobe; neuromuscular junction; *Drosophila*

Introduction

Synapses in the brain facilitate the exchange of information from one neuron to another, culminating in integrated signals that inform the complex computations underlying movement and stimulus sensation. The presynaptic side of the synapse is defined by the active zone, a structural site comprised of quantal release machinery that anchors calcium channels near synaptic vesicles containing neurotransmitter (Wagh *et al.* 2006; Südhof 2012; Ehmann *et al.* 2018). After an influx of calcium through active zone-associated channels following an action potential, neurotransmitter is released into the synaptic cleft where it binds to cognate neurotransmitter receptors on the postsynaptic membrane (Lin and Goodman 1994; Siddiqui and Craig 2011; Wilson 2013; Mosca and Luo 2014; de Ramon Francàs *et al.* 2017). The activation of postsynaptic receptors propagates the signal from the presynaptic neuron to the postsynaptic cell. In the absence of active zones, synaptic communication is drastically impaired or blocked, and function is abrogated. Therefore, the specialized sites of communication between neurons must develop correctly over a specific timeframe and maintain their precise organization

throughout an organism's life to ensure that synaptic function continues unabated and retains aspects of synaptic plasticity necessary for appropriate behavioral coordination (Waites *et al.* 2005; Silbereis *et al.* 2016; Farhy-Tselnicker and Allen 2018; Aimino *et al.* 2023). Defects in the development of active zones (both in number and organization) have been found to underlie neurodevelopmental, neuropsychiatric, and even neurodegenerative diseases including autism and schizophrenia, demonstrating the necessity for understanding how synapses develop and organize at the circuit level (Bennett 2011; Grant 2012; Bonansco and Fuenzalida 2016; Mullins *et al.* 2016).

In the central nervous system especially, the high density of synaptic connections and concomitant difficulties of discerning the specific cell or cell type to which an active zone localizes makes the study of synapses with cell-type-specific resolution a challenge. As such, studies using antibodies to active zone machinery are limited in their utility for asking cell-type-specific questions as they recognize synapses in all cells that express active zone proteins *in vivo*. To better discern how synapses develop and change over time with cell-type specificity, genetic strategies using binary expression systems and transgenic active zone labels

Received on 14 July 2023; accepted on 17 September 2023

© The Author(s) 2023. Published by Oxford University Press on behalf of The Genetics Society of America.

This is an Open Access article distributed under the terms of the Creative Commons Attribution License (<https://creativecommons.org/licenses/by/4.0/>), which permits unrestricted reuse, distribution, and reproduction in any medium, provided the original work is properly cited.

have become powerful for studying synaptic organization in identified cell types with high resolution. Work in *Drosophila* especially has contributed greatly to the study of synaptic organization due to the wide variety of genetic tools available for experimental use in synaptic and neuronal labeling (Duhart and Mosca 2022). In recent years, our understanding of synaptic biology has markedly advanced through the study of the active zone protein Bruchpilot, the ortholog of vertebrate ELKS/CAST (Ohtsuka et al. 2002), which is an essential presynaptic component at both peripheral and central synapses in the fly (Ohtsuka et al. 2002; Wang et al. 2002; Wagh et al. 2006; Fouquet et al. 2009; Südhof 2012). In particular, the transgenic construct, Bruchpilot-Short (Fouquet et al. 2009), a truncated version of Bruchpilot that colocalizes with endogenous full-length Bruchpilot, is frequently used to study synaptic organization in specific cell types via binary expression systems like UAS/GAL4 (Kremer et al. 2010; Berger-Müller et al. 2013; Mosca and Luo 2014; Sugie et al. 2015; Coates et al. 2017, 2020; Mosca et al. 2017; Duhart and Mosca 2022; Aimino et al. 2023). When Bruchpilot-Short is conjugated to a fluorescent tag and visualized using confocal microscopy, the resultant protein appears as puncta that can be quantified and acts as a proxy measurement for the number of synapses within a specific brain region without interfering with the function or localization of endogenous Bruchpilot or adding ectopic synapses (Wagh et al. 2006; Fouquet et al. 2009; Kremer et al. 2010; Christiansen et al. 2011; Mosca and Luo 2014; Coates et al. 2017, 2020; Mosca et al. 2017; Aimino et al. 2023). Use of Bruchpilot-Short has led to novel discoveries about the development and organization of synapses (Fouquet et al. 2009; Kremer et al. 2010; Christiansen et al. 2011; Berger-Müller et al. 2013; Mosca and Luo 2014; Coates et al. 2017, 2020; Mosca et al. 2017; Aimino et al. 2023; Parisi et al. 2023), demonstrating its effectiveness as a reagent. Bruchpilot-Short is frequently used in conjunction with other synaptic and cellular transgenic constructs to label other synaptic components, including synaptic vesicles (Estes et al. 2000; Zhang et al. 2002; Williams et al. 2019; Certel, McCabe, et al. 2022; Certel, Ruchti, et al. 2022), other active zone components (Fouquet et al. 2009; Liu et al. 2011; Mosca et al. 2017; Fulterer et al. 2018; Özel et al. 2019), general cellular architecture (Lee and Luo 1999; Potter et al. 2010; Venken, Simpson, et al. 2011), and postsynaptic sites (Sánchez-Soriano et al. 2005; Leiss, Groh, et al. 2009; Leiss, Koper, et al. 2009; Kremer et al. 2010; Nicolai et al. 2010; Andlauer et al. 2014; Mosca and Luo 2014; Mosca et al. 2017; Fendl et al. 2020; Parisi et al. 2023). One such construct, mCD8-GFP (Lee et al. 1999), is a membrane-bound GFP tag that, when expressed in any cell type, labels the membranes of that cell, revealing its architecture. When expressed in a particular population of neurons under the control of a binary expression system, mCD8-GFP serves as a general neurite label for both dendrites and axons. Just as Bruchpilot-Short puncta can be quantified as a proxy for the number of synaptic contacts (Fouquet et al. 2009; Kremer et al. 2010; Christiansen et al. 2011; Berger-Müller et al. 2013; Mosca and Luo 2014; Coates et al. 2017, 2020; Mosca et al. 2017; Aimino et al. 2023; Parisi et al. 2023), membrane markers like mCD8-GFP can be quantified to determine the total volume of neurite membrane in a defined population of neurons (Mosca and Luo 2014; Mosca et al. 2017; Aimino et al. 2023). Together with Bruchpilot-Short, quantification of puncta number and neurite volume can be expressed as synaptic density within that neuronal population (Mosca and Luo 2014; Mosca et al. 2017; Aimino et al. 2023). Thus, employing constructs like Bruchpilot-Short-mStraw and mCD8-GFP together makes it possible to ask vital questions about the formation and organization of synapses within a defined population of neurons, thus

overcoming previous challenges brought about by the density of synaptic populations in vivo in the central nervous system.

To quantify metrics like synaptic density, it is necessary to express multiple effector or reporter constructs in vivo in tandem as synaptic density is the measure of the number of synaptic puncta within a given volume of neuronal membrane. While increasing the number of simultaneously expressed transgenes enables more complex experimentation, it also carries drawbacks. In cultured cells, multiple plasmids must be cotransfected, potentially resulting in cells that do not incorporate every plasmid that is transfected (González et al. 2011). Similarly, driving expression of multiple genes with a binary expression system like GAL4/UAS can lead to a dilution of transgene expression, causing effectors and reporters to not function optimally or sufficiently (Brand and Perrimon 1993). Oftentimes, multiple transgenes encoding different effectors and reporters are recombined onto the same chromosome to reduce the number of chromosomes that must be accounted for in the genetic crosses that enable certain experiments. However, this is often time-consuming and challenging, depending on the chromosomal position of each transgene. Further, though it may enable the introduction of additional transgenes and reduce the difficulty of the genetic crosses needed to create the experimental animal, recombination does not reduce the genetic load of the system. Additionally, viral technologies, including AAV-based vectors such as those used in studies of neuronal circuit tracing or as vectors for gene therapy (Naso et al. 2017; Weinholtz and Castle 2021), are often limited by the amount of genetic material that can be introduced inside a single viral particle (Grieger and Samulski 2005; Wu et al. 2010). As a result, strategies are needed not only to reduce the size of genetic material introduced but also to increase the likelihood of introducing all desired transgenic components with a decreased risk of dilution and failed or weakened expression. One approach to mitigating such drawbacks is to express a single open reading frame that can encode multiple gene products. Initially, internal ribosome entry site (IRES) sequences were used to promote the internal initiation of translation of 2 separate proteins (Martinez-Salas 1999; Douin et al. 2004). However, these sequences were limited in their effectiveness as the peptide following the IRES sequence would often have decreased expression compared to the preceding peptide (Kaufman et al. 1991; Ye et al. 1997; Mizuguchi et al. 2000; Underhill et al. 2007). More recent work employs 2A viral peptides, which are highly efficient ribosomal skipping peptides (Luke et al. 2009; Kim et al. 2011; Diao and White 2012; Daniels et al. 2014). When incorporated into a particular mRNA, the 2A peptide sequence serves as a skipping site, allowing the ribosome to separate from the mRNA, completing translation of the first sequence, and then re-entering the mRNA at the beginning of the second sequence, starting translation anew and producing a second product. As a result, placing the sequence of a 2A peptide between 2 complete sequences enables 1 continuous mRNA to code for 2 or more polypeptides of interest from a single promoter (Tang et al. 2009; Kim et al. 2011; Daniels et al. 2014). Previous work has indicated that constructs containing 2A peptides are less likely to show the decreased expression of the second protein product, as seen with IRES-containing constructs (Hasegawa et al. 2007; Leisegang et al. 2008). This approach can decrease the genetic load on a particular system, as now only 1 transgene ensures the expression of multiple products.

In *Drosophila*, there is a multitude of binary expression system drivers (GAL4, lexA, and QF) available, enabling tissue-specific expression in nearly any desired nervous system region and cell type. However, there is considerable variability in the expression

strength of binary expression system driver lines, such that not all driver lines can enable transgene expression equivalently. Some cell-type-specific GAL4 lines are weakly expressing, making it difficult to express multiple UAS transgenes simultaneously for concurrent labeling of multiple targets. As progressively more UAS transgenes are incorporated into an experimental design, the consistent translation of each transgene by a weak GAL4 is less likely, which can result in poor or even failed expression of each respective effector or label. To overcome this expression issue and enable expression of multiple neural markers via a single transgenic construct, we used a vector that contains the 2A peptide from the porcine teschovirus-1 (P2A) coding sequence (Daniels et al. 2014) to create a single transgenic construct that encodes both mCD8-GFP and Bruchpilot-Short-mStrawberry (Brp-Short-mStraw) from the same coding sequence. This new construct makes it possible to simultaneously express both neuronal labels from a single ORF rather than 2 independent ORFs (as with 2 independent UAS constructs) while concurrently reducing the genetic load on the system. Therefore, even weakly expressing GAL4s would be able to drive expression of both proteins with high signal fidelity as there would be fewer total transgenes being driven. As the independent constructs fluorescently label synapses as well as the neuronal membrane for visualization at the level of light microscopy, we have named the tool SynLight, a portmanteau of synapse and light. We designed versions of SynLight that can be driven via multiple binary expression systems, including the GAL4/UAS and QF/QUAS systems, making it possible to ask new questions about the development and organization of synapses throughout the nervous system with less concern over transgenic dilution or failed labeling. Here, we validate SynLight expression in multiple regions of the adult and larval nervous systems in *Drosophila*, including the olfactory, visual, and neuromuscular systems using both the GAL4/UAS and QF/QUAS systems. We additionally demonstrate that SynLight expression does not affect normal neuronal morphology; active zone puncta number as measurements from SynLight expression are quantitatively indistinguishable from measurements via independent Brp-Short-mStraw or mCD8-GFP transgene expression as well as endogenous Bruchpilot antibody staining. Thus, SynLight labels presynapses and neurite membranes, facilitating their visualization with high resolution and permitting more complex experimental design with reliable quantitative measurements. When expressed in a cell-type-specific manner using existing GAL4 or QF promoter lines, SynLight has a wide applicability to a variety of *Drosophila* nervous system regions and is a versatile tool for studying synaptic development and organization.

Materials and methods

Fly stocks and care

All control lines and genetic fly stocks were maintained on cornmeal: dextrose medium (Archon Scientific, Durham, NC, USA) at 21°C while crosses were raised on similar medium at 25°C (unless noted in the text) in incubators (Darwin Chambers, St. Louis, MO, USA) at 60% relative humidity with a 12/12 light/dark cycle.

Transgenes were maintained over balancers with fluorescent markers and visible phenotypic traits to allow for the selection of adults and larvae of the desired genotype. To drive expression in specific classes of CNS neurons, we used the following GAL4 or QF expression lines: *Or47b-GAL4* (Vosshall et al. 2000), *Or67d-GAL4* (Stockinger et al. 2005), *Or67d-QF* (Liang et al. 2013), *Mz19-GAL4* (Jefferis et al. 2003), *NP3056-GAL4* (Chou et al. 2010), *DIP-γ-GAL4* (Carrillo et al. 2015), and *27B03-GAL4* (Jenett et al. 2012). Expression at the neuromuscular junction (NM) was

achieved via *elav^{C155}-GAL4* (Lin and Goodman 1994) and *n-syb-QF* (Riabinina et al. 2015). The following UAS transgenes were used as synaptic labels or to express molecular constructs for genetic perturbation experiments: *UAS-Brp-Short-mStraw* (Fouquet et al. 2009; Mosca and Luo 2014), *UAS-mCD8-GFP* (Lee and Luo 1999), *UAS-SynLight* (*UAS-mCD8-GFP-P2A-Brp-Short-mStraw*; this study). Genotypes for each experiment are listed by figure panel in Table 1.

Cloning of SynLight plasmid and transgenic lines

Using restriction enzyme cloning, we first inserted the mCD8-GFP sequence (from pC-attB-bursa- α -mCD8-GFP-T2A-GAL4; a gift from Benjamin White) into a plasmid containing pC5-P2A-KAN (Daniels et al. 2014). We used BamHI and StuI as cut sites to put this sequence upstream of the P2A peptide sequence. We subsequently inserted the Bruchpilot-Short-mStrawberry sequence (pENTR-Brp-Short-mStraw; Mosca and Luo 2014), using NheI and AvrII as cut sites to position the sequence downstream of the P2A peptide and keep all sequences in the same frame of translation. mCD8-GFP-P2A-Bruchpilot-Short-mStrawberry was then migrated from the shuttle vector into a plasmid containing a pUAS-C5-attB sequence using restriction enzyme cloning with FseI and AscI as the cut sites (to ensure that all sequences remained in the same frame for translation) and ligated together to produce the final plasmid. A similar approach was used to engineer the QUAS version of the plasmid (pQUAST-Brp-Short-mStraw-attB; Mosca and Luo 2014). The final plasmid was sequence verified (GeneWiz, South Plainfield NJ), and the final construct sequence is available upon request. A Qiagen Maxi Prep kit (Qiagen, cat. no. 12163) was used to isolate donor plasmid DNA for the creation of transgenic fly lines. Transgenic flies (UAS and QUAS lines) were generated (BestGene, Chino Hills, CA, USA) with the construct integrated into the attP2 docking site (Groth et al. 2004) on the third chromosome. Subsequent transgenic flies (UAS line) were also generated (BestGene, Chino Hills, CA, USA) with the construct integrated

Table 1. Genotypes for each figure panel.

| Figure | Panel | Genotype |
|--------|-------|--|
| 1 | d | <i>w; Sp/+; UAS-mCD8-GFP-P2A-Brp-Short-mStraw/ NP3056-GAL4; +</i> |
| | e | <i>elav^{C155}-GAL4/w; CyO/+;</i> |
| | f | <i>UAS-mCD8-GFP-P2A-Brp-Short-mStraw/+; + w; +; QUAS-mCD8-GFP-P2A-Brp-Short-mStraw/ n-syb-QF2; +</i> |
| 2 | b-c | <i>w; Or47b-GAL4/UAS-Brp-Short-mStraw, UAS-mCD8-GFP; +; +</i> |
| | d-e | <i>w; Or47b-GAL4/+; UAS-mCD8-GFP-P2A-Brp-Short-mStraw/+; +</i> |
| 3 | b | <i>w; +; Or67d-GAL4, UAS-mCD8-GFP-P2A-Brp-Short-mStraw/+; +</i> |
| | c | <i>Or67d-QF/w; +; QUAS-mCD8-GFP-P2A-Brp-Short-mStraw/TM6b, Tb; +</i> |
| | d | <i>w; Mz19-GAL4/+; UAS-mCD8-GFP-P2A-Brp-Short-mStraw/+; +</i> |
| | e | <i>w; Sp/+; UAS-mCD8-GFP-P2A-Brp-Short-mStraw/ NP3056-GAL4; +</i> |
| 4 | a, d | <i>w; +; UAS-mCD8-GFP-P2A-Brp-Short-mStraw/ DIP-γ-GAL4; +</i> |
| | b | <i>w; +; UAS-mCD8-GFP-P2A-Brp-Short-mStraw/ 27B03-GAL4; +</i> |
| 5 | a | <i>elav^{C155}-GAL4/w; Pin or Cyo/+; +; +</i> |
| | b, c | <i>elav^{C155}-GAL4/w; Pin or Cyo/+;</i> |
| | d | <i>UAS-mCD8-GFP-P2A-Brp-Short-mStraw/+; + w; +; QUAS-mCD8-GFP-P2A-Brp-Short-mStraw/ n-syb-QF2; +</i> |

into the VK00037 docking site (Venken et al. 2006) on the second chromosome. After transgenic fly stocks were obtained, construct integration was verified visually by the incorporation of a copy of *mini-white* gene allowing us to identify successful transformants via changes in eye color, as consistent with established transgenic protocols (Brand and Perrimon 1993; Venken, Schulze et al. 2011). When the lines were subsequently utilized for experiments, we did not visually observe differences in expression or localization of each marker between the UAS transgenes on the second and third chromosomes. As such, for all subsequent experiments, we used the construct on the third chromosome.

Immunocytochemistry

Adult flies were cleared from vials 1 day before collection and on the following day, newly eclosed adults were chosen based on genotype using identifiable balancers and phenotypic markers. Flies were then aged ten days before dissection and immunostaining. Brains were fixed in 4% paraformaldehyde for 20 min before being washed in phosphate buffer (1× PB) with 0.3% Triton (PBT). Brains were then blocked for an hour in PBT containing 5% normal goat serum (NGS) before being incubated in primary antibodies diluted in PBT with 5% NGS for 2 days at 4°C. Following staining, primary antibodies were discarded and the brains washed 3 × 20 min with PBT and incubated in secondary antibodies diluted in PBT with 5% NGS for an additional 2 days at 4°C. The secondary antibodies were then discarded; the brains were washed 3 × 20 min in PBT and then incubated overnight in SlowFade (Thermo Fisher Scientific, Waltham, MA, USA) gold antifade mounting media and allowed to sink. Brains were then mounted in SlowFade mounting media using a bridge-mount method with no. 1 cover glass shards and stored at 20°C before being imaged (Wu and Luo 2006).

Larvae were processed for immunocytochemistry as previously described (Mosca and Schwarz 2010; Restrepo et al. 2022). Larvae were grown in population cages on grape plates with yeast paste until they reached wandering third instar stage. Larval fillet dissections were done in Ca²⁺-free modified *Drosophila* saline, and then fillets were fixed in 4% paraformaldehyde in phosphate-buffered saline (PBS) for 20 min. Samples were then washed with PBS with 0.3% Triton (PBST) for 1 h at room temperature. The fillets were blocked with PBST containing 5% NGS for 1 h at room temperature and then incubated in primary antibodies diluted in PBST with 5% NGS overnight at 4°C. The following day, primary antibodies were discarded, and then fillets were washed with PBST for 3 × 10 min before being placed in secondary antibodies diluted in PBST with 5% NGS for 2 h at room temperature. Fillets were then washed again 5 × 15 min in PBST before being mounted in Vectashield (Vector Laboratories). Samples were stored at 4°C before being imaged.

The following primary antibodies were used: mouse anti-Nc82 (DSHB, cat. no. mAbnc-82, 1:250; Laissue et al. 1999), rabbit anti-DsRed (TaKaRa Bio, cat. no. 632496, 1:250; Mosca and Luo 2014), chicken anti-GFP (Aves, cat. no. GFP-1020, 1:1,000; Mosca and Luo 2014), rat anti-N-Cadherin (DSHB, cat. no. mAbDNEX-8, 1:40; Hummel and Zipursky 2004), and Alexa647-conjugated goat anti-HRP (Jackson ImmunoResearch, cat. no. 123-605-021, 1:100; Jan and Jan 1982). Alexa488- (Jackson ImmunoResearch, West Grove, PA, USA), Alexa568- (Thermo Fisher Scientific, Waltham, MA, USA), and Alexa647-conjugated (Jackson ImmunoResearch, West Grove, PA, USA) secondary antibodies were used at 1:250 while FITC-conjugated (Jackson ImmunoResearch, West Grove, PA, USA) secondary antibodies were used at 1:200. In some cases, nonspecific background is recognized by the dsRed antibodies (in

the form of large red spots appear around the antennal lobes and outside of the tissue observed). These are part of the background, are not caused by any of the transgenic constructs used (Mosca and Luo 2014), and did not influence any quantification or scoring methods (see below). Additionally, large, bright objects around the antennal lobes can be seen when visualizing projection neurons (PNs) and local interneurons (LNs). These objects correspond to the cell bodies of the neurons being imaged and are likely due to Brp-Short-mStraw beginning to colocalize with endogenous Bruchpilot as it is being synthesized in the ER as well as membrane-bound GFP. This is a known phenomenon associated with Bruchpilot-Short, and as such, these objects are excluded during analysis and do not influence any quantification (see below).

Imaging and analysis

All images of adult brains were obtained using a Zeiss LSM880 Laser Scanning Confocal Microscope (Carl Zeiss, Oberlochen, Germany) using a 20× 0.8 NA Plan-Apochromat lens, 40× 1.4 NA Plan-Apochromat lens, or a 63× 1.4 NA Plan-Apochromat f/ELYRA lens at an optical zoom of 3×. Images of third instar larval NMJs were obtained using the same confocal microscope using a 40× 1.4 NA Plan-Apochromat lens or a 63× 1.4 NA Plan-Apochromat f/ELYRA lens. Images were centered on the glomerulus or NMJs of interest, and the z-boundaries were set based on the appearance of the synaptic labels, Brp-Short-mStraw or mCD8-GFP. Images were analyzed 3 dimensionally using the Imaris Software 9.7.1 (Oxford Instruments, Abingdon, UK) on a custom-built image processing computer (Digital Storm, Fremont, CA, USA) following previously established methods (Aimino et al. 2023). For both adult brains and larval NMJs, Brp-Short-mStraw and endogenous Brp puncta were quantified using the “Spots” function with a spot size of 0.6 μm. Neurite volume was quantified using the “Surfaces” function with a local contrast of 3 μm and smoothing of 0.2 μm for *Or47b* olfactory receptor neurons (ORNs). The resultant masks were then visually inspected to ensure their conformation to immunostaining.

Quantitative measurement and statistical analyses

All data were analyzed using Prism 8 (GraphPad Software, Inc., La Jolla, CA, USA). This software was also used to generate graphical representations of data. Unpaired Student’s t-tests were used to determine significance between 2 groups while paired Student’s t-tests were used to determine the significance between puncta numbers for individual NMJs. One-way ANOVA with Tukey’s multiple comparisons tests was used to determine significance between groups of 3 or more. A P-value of 0.05 was set as the threshold for significance in all studies. For measurements of signal colocalization, Pearson’s coefficients and Manders’ split coefficients were obtained using the JACoP: Just Another Co-localization Plugin for ImageJ (Bolte and Cordelières 2006). For each figure, informative genotypes have been presented along with controls appropriate for each genotype.

Results

SynLight is designed to label active zones and neurite membranes in the same cell population

Established approaches in *Drosophila* to examine synapse density in particular classes of neurons typically involve expressing 2 constructs: (1) Brp-Short-mStraw to label active zones made by the neurons and (2) mCD8-GFP (or an equivalent) to label the processes of neurons (Fouquet et al. 2009; Kremer et al. 2010; Christiansen et al. 2011; Berger-Müller et al. 2013; Mosca and Luo

2014; Sugie et al. 2015; Coates et al. 2017, 2020; Mosca et al. 2017; Aimino et al. 2023; Parisi et al. 2023). Previous work established that 2A peptide approaches work efficiently in *Drosophila* for encoding multiple proteins from a single ORF (Diao and White 2012; Daniels et al. 2014). Therefore, we designed and built a single construct containing Brp-Short-mStraw and mCD8-GFP separated by a 2A peptide and named it SynLight. SynLight takes advantage of P2A, a viral 2A peptide from porcine teschovirus-1 (Kim et al. 2011; Daniels et al. 2014). The P2A protein is derived from a ribosomal skipping protein that allows multiple separate proteins to be made from a single mRNA (Tang et al. 2009; Kim et al. 2011). Using a vector that contains the P2A coding sequence, multiple cloning sites, and restriction sites (Le et al. 2007; Daniels et al. 2014), we engineered a single transgene that produces multiple proteins from a single coding sequence via restriction cloning (Fig. 1a). The resultant vector contained mCD8-GFP inserted into the first restriction site and Brp-Short-mStraw inserted into the second site with the 2 separated by P2A, producing mCD8-GFP-P2A-Brp-Short-mStraw (Fig. 1b). From the single mRNA produced by the transgene following activation by a promoter driver line, 2 separate proteins would be produced, Brp-Short-mStraw and mCD8-GFP (Fig. 1c). We engineered both UAS and QUAS versions of SynLight and established transgenic lines on the third chromosome in the attP2 site (Groth et al. 2004) so that the construct could be used with multiple binary expression systems. We subsequently established a transgenic line on the second chromosome in the VK00037 site (Venken et al. 2006). When SynLight was expressed in olfactory neurons of the adult brain using NP3056-GAL4 (Fig. 1d–d’); Chou et al. 2010) or pan-neuronally using *elav*^{CI55}-GAL4 (Fig. 1e–e’; Lin and Goodman 1994) after immunohistochemical staining for Brp-Short-mStraw and mCD8-GFP as established previously (Mosca and Luo 2014; Mosca et al. 2017; Aimino et al. 2023), we observed clear, subcellularly distinct signal for both Brp-Short-mStraw and mCD8-GFP. We obtained similar findings when SynLight was expressed in the ventral nerve cord of third instar larvae using the pan-neuronal QF driver *n-syb-QF* and visualized using the native fluorescence of both labels (Fig. 1f–f’; Riabinina et al. 2015). For both the central and peripheral nervous systems, these data demonstrated that there was separation between the 2 products and indicated that ribosomal skipping occurred successfully during translation, resulting in the synthesis of Brp-Short-mStraw and mCD8-GFP separately (insufficient separation would manifest as precise overlap between the mCD8-GFP and Brp-Short-mStraw channels). With the successful establishment of transgenic UAS- and QUAS-SynLight lines, we further sought to validate the construct as a synaptic labeling and quantification method.

Quantification of synapses and neuronal morphology in antennal lobe neurons using SynLight

Both Brp-Short-mStraw and mCD8-GFP have enabled quantitative analyses of synaptic organization at peripheral and central synapses, resulting in established measurements of synapse number and neurite volume, especially in the olfactory system (Kremer et al. 2010; Christiansen et al. 2011; Mosca and Luo 2014; Mosca et al. 2017; Aimino et al. 2023). As such, there is a rich history of control data against which we can benchmark SynLight performance. To demonstrate the utility of SynLight for making quantitative measurements of synapse organization and density, we first turned to ORNs in the *Drosophila* antennal lobe. In the antennal lobe, ORNs, PNs, and LNs are the 3 major neuron types that

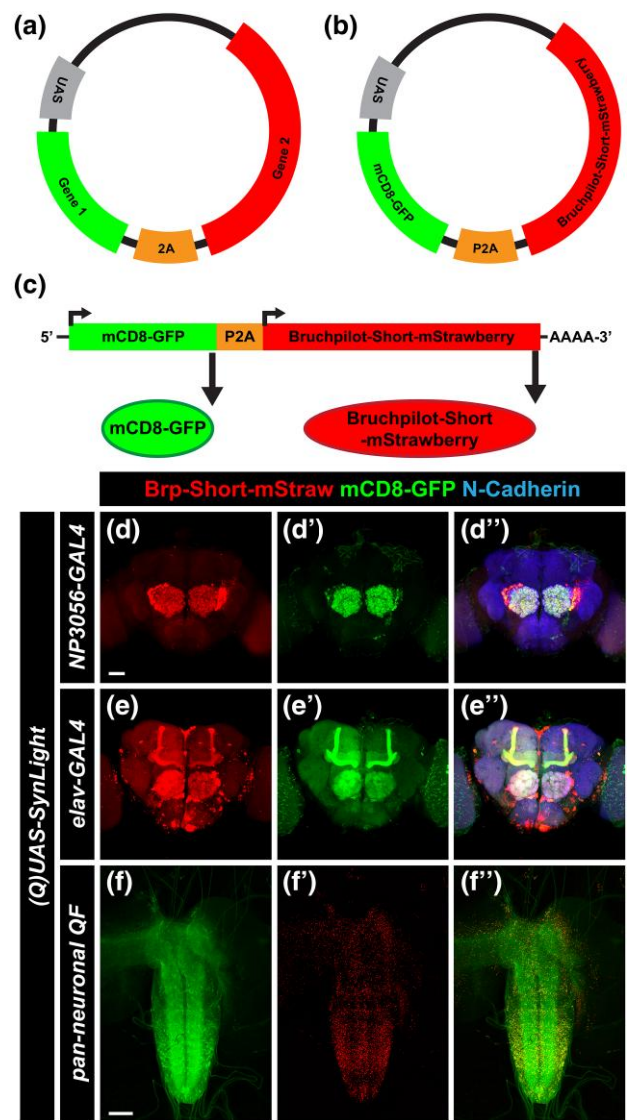


Fig. 1. Strategy for generating SynLight, a single transgene that expresses both membrane-tagged GFP and mStrawberry-tagged Bruchpilot-Short. a) Diagram of an example plasmid containing a UAS vector and codon-optimized 2A peptide coding sequence (Daniels et al. 2014). Flanking either side of 2A is multiple cloning sites and restriction sites that facilitate insertion of 2 or more genes of interest. b) Diagram of the SynLight plasmid. Using restriction enzymes, the mCD8-GFP coding sequence was inserted preceding the P2A coding sequence, and then the Bruchpilot-Short-mStrawberry coding sequence was inserted following the P2A sequence, keeping all sequences in frame. c) Diagram of SynLight mRNA, showing 2 separate proteins being produced from a single mRNA sequence. d–d’’) Representative maximum projection confocal image stacks of multiglomerular LNs of the adult brain expressing SynLight and stained with antibodies against mStraw (d), GFP (d’), and N-Cadherin (merge, d’). These images show overlapping, yet distinctly different subcellular localization of Brp-Short-mStraw and mCD8-GFP. e–e’’) Representative maximum projection confocal image stacks of SynLight being driven pan-neuronally in the adult brain and stained with antibodies as in d. Again, these images show overlapping, yet distinct subcellular localization of Brp-Short-mStraw and mCD8-GFP. f–f’’) Representative maximum projection confocal image of the third instar ventral nerve cord expressing SynLight, showing separate endogenous expression of Brp-Short-mStraw (f) and mCD8-GFP (f’’) via the native fluorescence from the mStrawberry and GFP fluorophores. Scale bars = 40 μm (d–e); 80 μm (f).

contribute to the sensation and subsequent relay of olfactory information to higher-order brain structures such as the mushroom bodies and the lateral horn (Vosshall et al. 2000; Jefferis et al. 2001;

Tanaka et al. 2009). ORNs, PNs, and LNs each project to the roughly 50 glomeruli that comprise the antennal lobe, which are subdivided based on the type of olfactory information they receive, and form synapses with each other to create functional circuits (Suh et al. 2004; Hallem and Carlson 2006; Jefferis et al. 2007; Grabe and Sachse 2018).

We first examined ORNs of the VA11m glomerulus (Fig. 2a) using *Or47b-GAL4* (Vosshall et al. 2000) and compared expression of independent Brp-Short-mStraw and membrane-bound GFP transgenes (Fig. 2b–c') to SynLight (Fig. 2d–e') following immunohistochemical staining for Brp-Short-mStraw and mCD8-GFP. Qualitatively, expression patterns and subcellular localization of SynLight vs mCD8-GFP/Brp-Short-mStraw from independent transgenes were indistinguishable from one another regardless of genotype. Subsequently, for each genotype, we quantified Brp-Short-mStraw puncta and neurite volume (as represented by mCD8-GFP staining) and found that Brp-Short-mStraw puncta number (Fig. 2f) and neurite volume (Fig. 2g) in VA11m ORNs were not significantly different between flies expressing SynLight and those expressing Brp-Short-mStraw and mCD8-GFP independently. We then calculated synapse density (Fig. 2h) by dividing the Brp-Short-mStraw puncta number by the neurite volume for each individual glomerulus and continued to find no significant difference between ORNs expressing SynLight and those expressing Brp-Short-mStraw and mCD8-GFP independently. This indicates that SynLight accurately recapitulates independent Brp-Short and mCD8-GFP expression both qualitatively and quantitatively. Moreover, SynLight expression does not interfere with synaptic organization or development of individual neuron types, as the mature synapse number and volume are unaltered when compared to published data (Mosca and Luo 2014; Mosca et al. 2017; Aimino et al. 2023). Therefore, SynLight is a viable strategy for quantitatively assessing synaptic organization with fewer genetic transgenes.

Having established that SynLight is robustly expressed in antennal lobe VA11m ORNs without affecting synaptic organization, we next expanded our analysis by driving SynLight expression in multiple cell types of the olfactory system (Fig. 3a). When driven in a different population of antennal lobe ORNs using *Or67d-GAL4* (DA1 ORNs; Stockinger et al. 2005) or *Or67d-QF* (Liang et al. 2013), we saw robust labeling of ORN active zones and neurites (Fig. 3b–c'). We also examined SynLight expression in other antennal lobe neurons beyond ORNs: we used *Mz19-GAL4* (Jefferis et al. 2003) and *NP3056-GAL4* (Chou et al. 2010) to drive SynLight expression in DA1 PNs (Fig. 3d–d') and multiglomerular LNs of DA1 (Fig. 3e–e'), respectively. As with DA1 ORNs, we found that SynLight labels active zones and neurites in both classes of neurons and that the labeling is consistent with previous results from the same drivers (Mosca and Luo 2014; Aimino et al. 2023). Taken together, SynLight expression is evident regardless of the olfactory neuron class in which it is expressed or via which binary expression system it is driven, further demonstrating its utility as a tool for studying synapse formation and organization.

SynLight labels presynaptic connections in neurons of the visual system

To expand our study of SynLight expression beyond the olfactory system, we next examined the fly visual system. Both the anatomy and organization of the fly visual system have been well characterized (Takemura et al. 2013, 2015; Yang and Clandinin 2018; Scheffer et al. 2020; Choi et al. 2021), and the fly visual system represents an excellent model for studying synaptic development and organization (Clandinin and Zipursky 2002) as well as visual processing

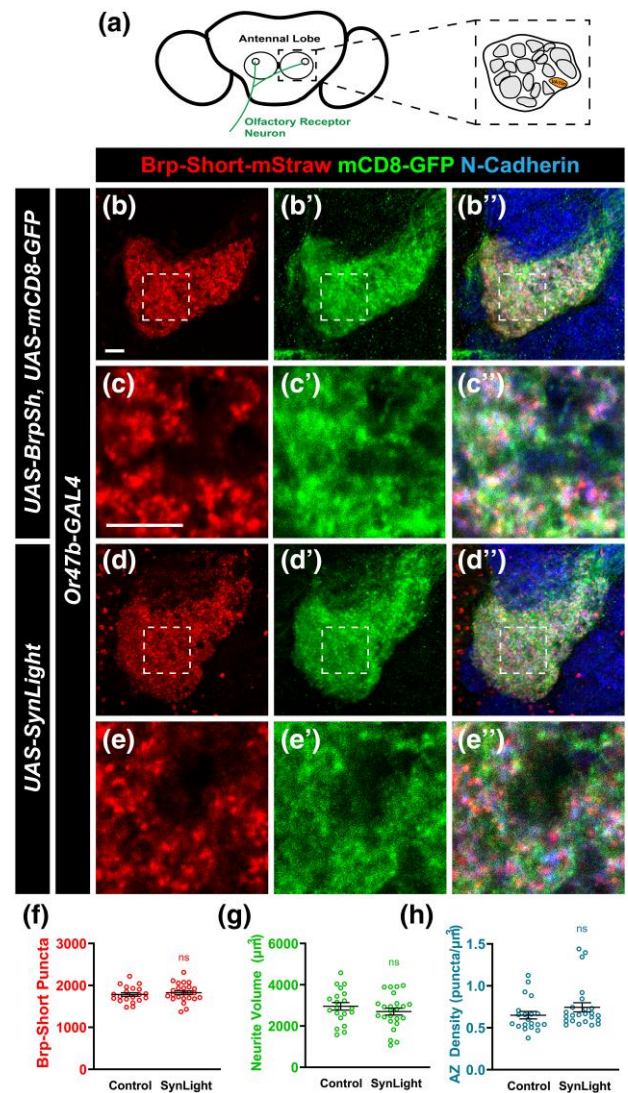


Fig. 2. SynLight expression does not affect synapse number in olfactory neurons. a) Diagram of the *Drosophila* antennal lobes showing ORNs (green) of the VA11m glomerulus (orange). b–b'') Representative confocal image stacks of 10-day-old male adult VA11m ORNs expressing Brp-Short-mStraw and membrane-tagged GFP separately and stained with antibodies against mStraw (b), GFP (b'), and N-Cadherin (merge, b''). c–c'') High-magnification, single optical image section of ORNs from inset in b showing colocalization, but not complete overlap, of synaptic labels. d–d'') Representative confocal image stacks of 10-day-old male adult VA11m ORNs expressing SynLight and stained with antibodies as in b. e–e'') High-magnification, single optical image section from inset in d also showing colocalization, but not complete overlap, consistent with subcellular localization and suggesting P2A-mediated cleavage is occurring successfully. f–h) Quantification of Brp-Short-mStraw puncta number (f), membrane GFP volume (g), and synapse density (h) for adult male VA11m ORNs expressing either SynLight or Brp-Short-mStraw and membrane-tagged GFP separately. Brp-Short-mStraw puncta number, neurite volume, and synapse density obtained using SynLight are not significantly different from using Brp-Short-mStraw and membrane-GFP separately. For each genotype, $n \geq 20$ glomeruli from 10 brains. n.s., not significant. Scale bars = 5 μm .

(Yang and Clandinin 2018). Further, tagged versions of Bruchpilot have been used extensively to characterize both the cellular events underlying and the molecular mechanisms supporting, synaptic plasticity in the visual system (Berger-Müller et al. 2013; Chen et al. 2014; Sugie et al. 2015; Shimozone et al. 2019; Araki et al. 2020; Kawamura et al. 2020; Duhart and Mosca 2022; Osaka et al. 2023),

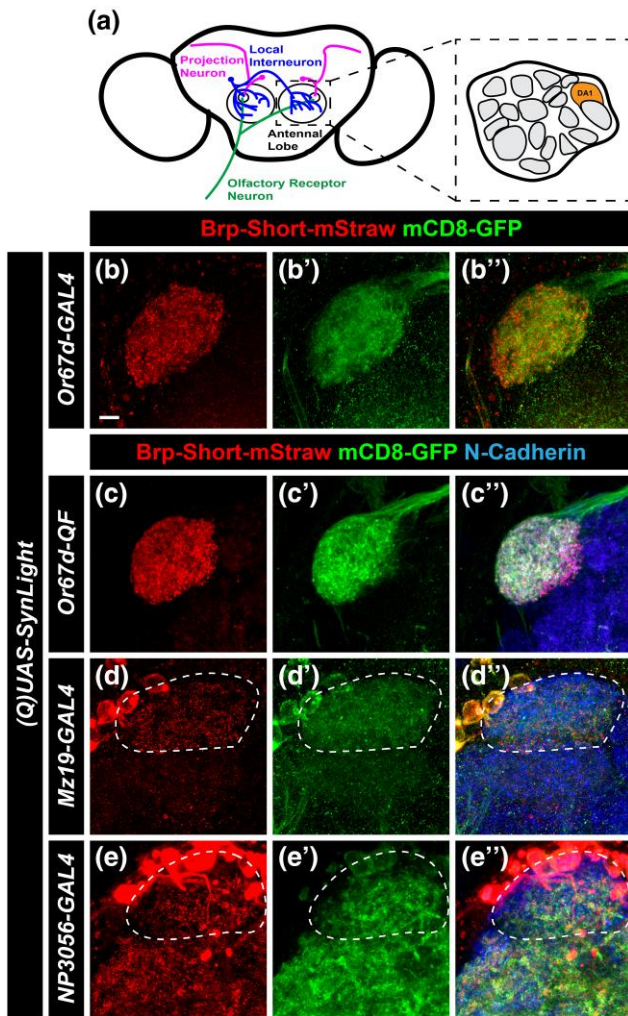


Fig. 3. SynLight labels presynaptic active zones and neuronal membranes in multiple cell types of the olfactory system. a) Diagram of the *Drosophila* antennal lobes showing ORNs (green), PNs (magenta), and multiglomerular LNs (blue) of the DA1 glomerulus (orange). b–c) Representative confocal image maximum projections of male adult DA1 ORNs expressing SynLight via a GAL4 (b) or QF (c) driver and stained with antibodies against mStraw (b, c), GFP (b', c'), and N-Cadherin (merge, b'', c''). d–e) Representative confocal image maximum projections of male adult DA1 PNs (dashed white lines) (d) and multiglomerular LNs (e) of the DA1 glomerulus (dashed white lines) expressing SynLight and stained with antibodies as in b–c. In e, multiglomerular LNs project throughout the antennal lobe but only the DA1 glomerulus is encircled for comparison. For each experimental group, $n \geq 5$ brains. Scale bar = 5 μm .

highlighting the utility of Brp-based labeling tools in understanding visual biology. To determine if SynLight could be used to concurrently label neuronal membranes and active zones in the visual system, we drove UAS-SynLight in the visual system using 2 different GAL4 drivers, *Dpr Interacting Protein- γ (DIP- γ)-GAL4* (Carrillo et al. 2015) and *27B03-GAL4* (Jenett et al. 2012) and examined both Brp-Short puncta and GFP-tagged neuronal membranes. *DIP- γ -GAL4* labels Dm8 neurons in layer M6 of the medulla (Fig. 4a–a') while *27B03-GAL4* drives expression in neurons of the optic lobe (Fig. 4b–b'). In both cases, we observed robust expression of SynLight and labeling consistent with release sites (via Brp-Short-mStraw) and general neuronal processes (via mCD8-GFP), indicating the efficacy and applicability of the SynLight construct beyond the olfactory system.

The Dm8 neurons labeled by *DIP- γ -GAL4* are postsynaptic to R7 photoreceptor neurons and form a connection analogous to the

ORN to PN synapses in the antennal lobe (Fig. 4c; Takemura et al. 2013). Processes of Dm8 neurons also form synaptic contacts onto Tm5c neurons, comprising a circuit that mediates UV preference (Karuppudurai et al. 2014). Both connections (R7 \rightarrow Dm8 and Dm8 \rightarrow Tm5c) form within the M6 layer of the medulla, suggesting that presynaptic R7 terminals should localize near (but not overlap with) Dm8 presynaptic terminals. We reasoned that concurrent labeling of R7 and Dm8 terminals would result in presynaptic staining of both neuron classes and that their respective presynaptic sites would be found in close proximity to one another within layer M6 of the medulla. To do so, we drove expression of SynLight in Dm8 neurons and costained the optic lobes with antibodies to Chaoptin, a marker for R7 photoreceptor cells (Krantz and Zipursky 1990). Indeed, when we specifically examined the M6 layer, we found that Dm8 Brp-Short puncta and R7 photoreceptor Chaoptin are present in similar regions of the optic lobe (Fig. 4d–d'). Furthermore, Dm8 Brp-Short-mStraw puncta and R7 Chaoptin signals do not overlap but are instead adjacent to one another as predicted (Fig. 4d''). Thus, SynLight expression can recapitulate expected patterns of synaptic organization in the visual system, indicating its utility as a synaptic label. Taken together with our findings from the olfactory system (Figs. 2 and 3), these data show that SynLight is a robust, reliable tool for concurrent labeling of synaptic active zones and general neuronal processes in multiple central nervous system populations.

SynLight accurately labels and quantifies active zones at neuromuscular synapses

To explore the utility of SynLight beyond the central nervous system, we next turned to peripheral NMJ synapses. NMJ synapses are highly stereotyped and are a long-studied, powerful system for uncovering active zone biology (Landgraf and Thor 2006; Menon et al. 2013; Chou et al. 2020) making them an optimal synapse for examining SynLight expression and quantification. We first expressed SynLight pan-neuronally via *elav^{C155}-GAL4* (Lin and Goodman 1994) and observed robust labeling of both general membranes (via mCD8-GFP) and active zones (via Brp-Short-mStraw) at NMJs (Fig. 5b–b') that was absent from non-expressing controls (Fig. 5a–a'). Consistently, mStraw-positive Brp-Short puncta labeled by SynLight overlapped with endogenous Bruchpilot antibody staining (Fig. 5c–c'), suggesting that SynLight labeling accurately revealed endogenous active zones. We further observed similar Brp-Short-mStraw and mCD8-GFP expression and localization with QUAS-SynLight (Fig. 5d–d') expression via *n-syb-QF* (Riabinina et al. 2015), indicating that multiple binary expression system versions of SynLight provide robust labels. Taken together, this indicates that SynLight is effectively and accurately expressed at NMJ synapses in separable pools reflecting membranes and release sites.

Having established that SynLight accurately localizes to NMJ synapses and membranes, we next assessed SynLight as a quantitative tool for active zone puncta. NMJ terminals have a characteristic number of active zone puncta when stained with antibodies to endogenous Bruchpilot, highlighting this metric as a reliable quantitative measurement of synaptic growth (Collins and DiAntonio 2007; Daniels et al. 2008; Wairkar et al. 2008). To determine if SynLight could be reliably used to quantify active zones, we counted Brp-Short-mStraw puncta at muscle 4 NMJ terminals and compared the data to counts of puncta recognized by the monoclonal antibody NC82 to endogenous Bruchpilot (Laissue et al. 1999; Wagh et al. 2006). There was no significant difference in the average puncta number visualized by mStraw (via SynLight) or NC82 (monoclonal antibody to Brp) staining (Fig. 5e), suggesting that SynLight could

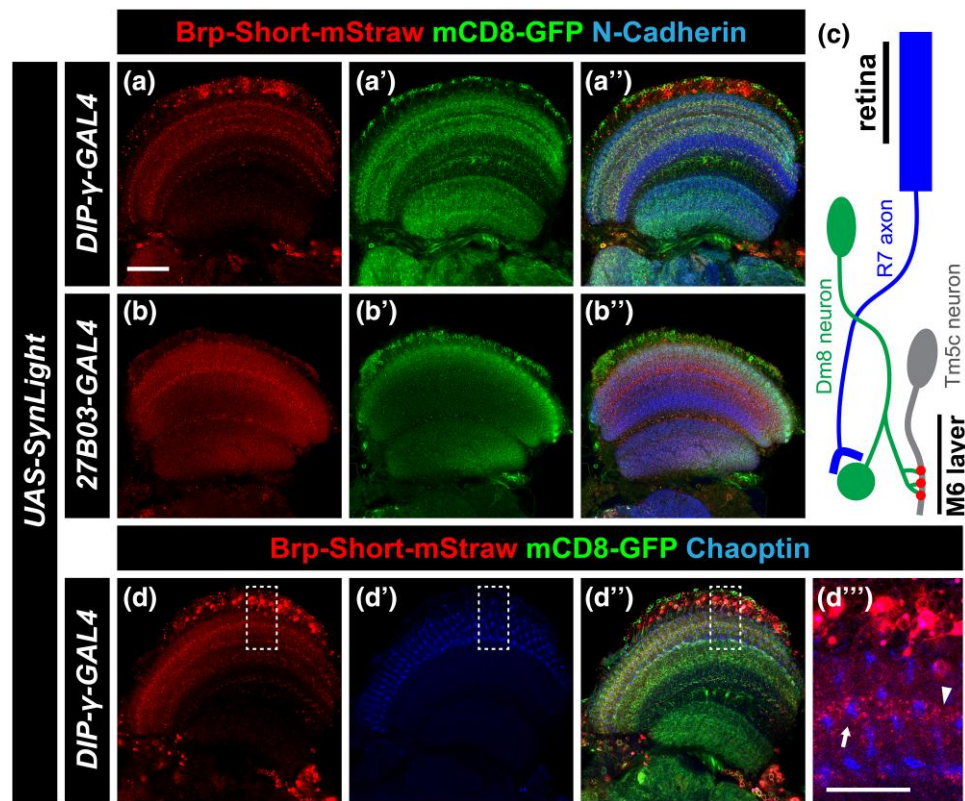


Fig. 4. SynLight labels presynaptic active zones and neuronal membranes in neurons of the visual system. a–b'') Representative single confocal image sections of male adult brains expressing SynLight using *DIP-γ-GAL4* to label Dm8 neurons a) or *27B03-GAL4* to label optic lobe neurons b) and stained with antibodies against mStraw (a, b), GFP (a', b'), and N-Cadherin (merge, a'', b''). c) Schematic showing the connections between R7 photoreceptor axons (labeled), Dm8 neurons (labeled), and Tm5c neurons (labeled). R7 axons project from the retina and synapse onto the dendrites of Dm8 neurons. Dm8 neurons subsequently form synapses with Tm5c neurons, forwarding the visual information received from R7 axons. The presynaptic active zones of Dm8 neurons (d) and axon terminals of R7 cells (d'') are both found in the M6 layer of the medulla. d–d'') Representative single confocal image sections of male adult brains expressing SynLight in Dm8 neurons and stained with antibodies against mStraw (d), GFP (merge, d'), and Chaoptin (d''). d'') Single, high-magnification image section from insets (dashed boxes, d) showing mStraw and Chaoptin costaining. Arrow indicates region of Brp-Short-mStraw and Chaoptin in close proximity while arrowhead indicates a region with only Brp-Short-mStraw. For each experimental group, $n \geq 5$ brains. Scale bars = 20 μm a); 10 μm (d'').

accurately quantify Brp-positive endogenous active zone number. To further validate our approach, we compared the individual Brp-Short-mStraw and NC82 puncta counts for each muscle 4 NMJ terminal to ensure that each metric gave the same result at the single NMJ being examined. Further, we observed no significant difference between the paired Brp-Short-mStraw and NC82 puncta number for each individual NMJ (Fig. 5f), demonstrating accurate and congruent reporting. To ensure that variants of SynLight for different binary expression systems (namely, GAL4 vs QF) function equivalently, we also compared Brp-Short-mStraw puncta number and NC82 puncta number between muscle 4 NMJ terminals expressing either *UAS-SynLight* or *QUAS-SynLight*. We found that there was no significant difference between the average Brp-Short-mStraw puncta number and the average NC82 puncta number (Fig. 5g), regardless of which SynLight variant was used to visualize these NMJs.

Although we observed no difference in average Brp-Short-mStraw or NC82 puncta number, we sought to further assess the utility of SynLight in accurately labeling presynaptic active zones using colocalization analysis. We analyzed signal colocalization between the Brp-Short-mStraw and NC82 channels for each individual muscle 4 NMJ terminal image used in Fig. 5c, e, and f. We plotted pixel intensity for each fluorescence signal and observed a positive correlation between NC82 signal and Brp-Short-mStraw signal (Fig. 5h), suggesting colocalization between the 2 labels. We also calculated both Pearson's and Manders' split coefficients for each muscle 4 NMJ terminal to more directly assess colocalization (Fig. 5i).

Pearson's coefficients range from 1 to -1 with a value of 1 indicating full colocalization and a value of -1 indicating no correlation between the 2 signals (Manders et al. 1993). Manders' coefficients range from 0 to 1 with a value of 1 indicating complete cooccurrence of pixel signal (Manders et al. 1993). For each muscle 4 NMJ terminal, we obtained positive Pearson's coefficients and Manders' coefficients close to 1, implying correlation of Brp-Short-mStraw and NC82 puncta signal and colocalization of our synaptic labels (Fig. 5i; average $P = 0.447$, average $M_1 = 0.746$, and average $M_2 = 0.53$). In all, the data indicate that SynLight accurately reports NMJ synaptic organization both qualitatively and quantitatively. Combined, our findings establish that SynLight functions as a robust synaptic label at both peripheral and central synapses in *Drosophila*.

Discussion

As technologies improve, making novel manipulations of, and labeling in, the nervous system possible, there is a growing need to incorporate more genetic components into experiments. Experiments in model organisms especially often have at least 3 transgenes (Venken, Schulze et al. 2011; Chou et al. 2020; Duhart and Mosca 2022) for even basic experiments: a genetic driver (e.g. GAL4, QF, *lexA*, and *Cre*), a reporter (GFP, synaptic labels, and receptor labels), and an effector (e.g. an optogenetic regulator of activity, toxin, endocytosis blocker, and kinase activity regulator). Multiple challenges exist, however, with such experiments.

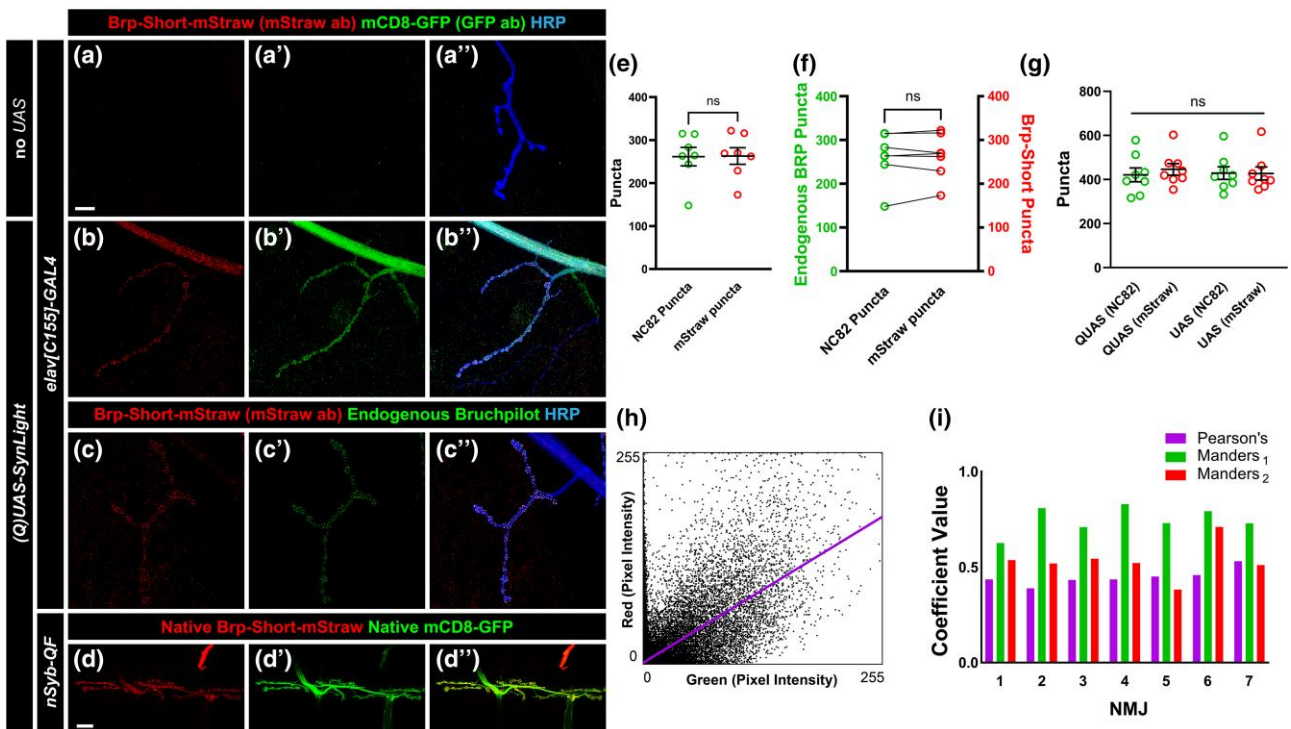


Fig. 5. SynLight labels the larval NMJ and does not alter synapse formation. a–b'') Representative confocal image maximum projections of muscle 4 NMJs in control a) or SynLight-expressing b) wandering third instar larvae stained with antibodies against mStraw (a, b), GFP (a', b'), and HRP (merge, a'', b''). The negative control lacking SynLight shows no mStraw or GFP immunoreactivity while pan-neuronal SynLight expression shows clear visibility of both markers. c–c'') Representative confocal image maximum projections of a muscle 4 NMJ expressing pan-neuronal SynLight and stained for antibodies against mStraw (c), NC82 (c''), and HRP (merge, c''). d–d'') Representative confocal image maximum projections of muscle 6/7 NMJs expressing SynLight showing endogenous expression of Brp-Short-mStraw (d) and mCD8-GFP (d'') via native fluorescence from the mStrawberry and GFP fluorophores. e) Quantification of active zone puncta visualized by antibody staining of endogenous Bruchpilot (via monoclonal antibody NC82) or expression of Brp-Short-mStraw via SynLight from c. There is no significant difference between Brp-Short-mStraw-positive and NC82-positive puncta. f) Quantification of active zone puncta as in e with paired comparisons for each individual NMJ. These data corroborate that, for each individual NMJ, there is no significant difference between Brp-Short-mStraw-positive and NC82-positive puncta number. g) Quantification of active zone puncta number visualized by antibody staining of endogenous Bruchpilot or expression of Brp-Short-mStraw via SynLight as in e for muscle 4 NMJ terminals expressing either QUAS-SynLight [QUAS (NC82) and QUAS (mStraw)] or UAS-SynLight [UAS (NC82) and UAS (mStraw)]. There is no significant difference between NC82 and Brp-Short-mStraw puncta number when either SynLight variant (QUAS or UAS) is used. h) Representative scatterplot of green pixel intensity (from NC82 puncta signal) and red pixel intensity (from Brp-Short-mStraw puncta signal) from a single muscle 4 NMJ terminal. Pearson's coefficient (first column in purple) shows a positive correlation between the 2 signals, suggesting colocalization. i) Correlation of active zone puncta visualized by antibody staining of endogenous Bruchpilot (via monoclonal antibody NC82) to active zone puncta expression of Brp-Short-mStraw via SynLight from each individual terminal in c. Correlations are represented by Pearson's coefficients (purple) or Manders' split coefficients (M_1 , second column in green; M_2 , third column in red). Positive Pearson's coefficient indicates positive correlation between NC82 puncta and Brp-Short-mStraw puncta. Values approaching 1 for Manders' coefficients indicate a similar correlation between the Brp-Short and NC82 signals. For each experimental group, $n \geq 7$ NMJs. n.s., not significant. Scale bars = 15 μ m a); 20 μ m d).

First, each transgene must be accounted for in genetic crosses to obtain experimental animals, leading to complex crosses where it is increasingly challenging to obtain "correct" progeny based on Mendelian ratios and unanticipated lethality. Second, genetic driver strength can be diluted by multiple transgenes (Brand and Perrimon 1993), leading to increased variability of expression and/or reduced efficacy of expressed transgenes. Finally, space constraints (from chromosome number or limits on viral DNA payload) can limit the number of genetic transgenes that can be present in the final experimental animal. Though some approaches like recombination of multiple transgenes onto the same chromosome can increase available genetic space for other transgenes and alleviate some of these concerns, recombinants do not reduce the total number of transgenes and the "genetic load" of the system persists. To begin to address some of these concerns, we developed a new strategy, SynLight, that uses the viral P2A ribosomal skipping peptide (Diao and White 2012; Daniels et al. 2014) to produce a single transgene that expresses both the membrane label mCD8-GFP (Lee et al. 1999) and the active zone label Brp-Short-mStraw (Fouquet et al. 2009; Mosca

and Luo 2014). We demonstrate that this strategy is effective in multiple central and peripheral neurons and is quantitatively similar to synaptic measurements using independent mCD8-GFP or Brp-Short-mStraw expression alone (Mosca and Luo 2014; Aimino et al. 2023). Using SynLight in either CNS or PNS experiments will enable more complex studies in vivo without sacrificing the number of labels possible.

To develop a construct for use in *Drosophila* that encodes both a presynaptic active zone marker as well as a neuronal membrane tag from a single sequence, we incorporated the P2A peptide, a ribosomal skipping sequence (Luke et al. 2009). This virus-derived peptide sequence mediates a skipping event during translation that enables the production of both proteins from a single mRNA (Tang et al. 2009; Kim et al. 2011; Daniels et al. 2014). We incorporated the established fly active zone label Brp-Short-mStraw (Kittel et al. 2006; Wagh et al. 2006; Fouquet et al. 2009; Kremer et al. 2010; Christiansen et al. 2011; Mosca and Luo 2014; Duhart and Mosca 2022; Aimino et al. 2023) and the general membrane marker mCD8-GFP (Lee et al. 1999) to produce a single SynLight transgene that concurrently labels all neuronal membranes via mCD8-GFP

and mature active zones via Brp-Short. We established multiple SynLight transgenic constructs (Fig. 1) on the second and third chromosomes for GAL4/UAS expression (Brand and Perrimon 1993) and on the third chromosome for QF/QUAS expression (Potter et al. 2010). We further demonstrated that SynLight is expressed with high fidelity in multiple classes of *Drosophila* CNS neurons, including those of the olfactory (Figs. 2 and 3) and visual (Fig. 4) systems. Further, the 2 products, mCD8-GFP and Brp-Short-mStraw, are readily separable in all neurons and, when quantified, produce similar results to established data and to expression of individual analogous constructs alone (Fig. 2). Thus, SynLight is effective for quantifying synapse density with only 1 construct, whereas previous experiments required 2 independent transgenes. We also demonstrated similar utility for SynLight at peripheral NMJ synapses. Not only is expression robust and labeling evident (Fig. 5) for membranes and active zones; measurements with SynLight accurately recapitulate data obtained from established antibodies to endogenous Bruchpilot (Laissue et al. 1999; Wagh et al. 2006). In all, SynLight accurately labels multiple subcellular structures via only 1 transgene.

Tools like SynLight will allow greatly increased utility within the fly nervous system. This will not only promote more complex and nuanced questions but also reduce experimental work. For example, to determine whether reduction of the function of a single gene influences synaptic density, 5 transgenes would optimally be required: a genetic GAL4/QF/lexA driver, an RNAi transgene to reduce specific gene function, Dcr2 to increase RNAi efficacy (Dietzl et al. 2007), mCD8-GFP (or an equivalent membrane marker) to measure neurite volume, and Brp-Short (or an equivalent active zone label) to quantify release sites. Not only is this a genetically complex experiment, but it may also reduce expression when a driver is used to express 4 independent transgenes. While the expression level tendered by strong drivers will enable the experiment, many circumstances will result in either reduced expression of the labels and/or reduced efficacy of the RNAi, leading to difficulty in interpreting the results. Previous approaches (Mosca et al. 2017; Aimino et al. 2023) have expressed the mCD8-GFP and Bruchpilot-Short transgenes in separate experiments, but as the measurements are then not taken from the same animal, synaptic density is not directly calculable. SynLight circumvents that issue by using only a single transgene to express both labels, thus increasing the utility of available experiments. Beyond simple perturbation experiments using a single class of neurons, SynLight also enables more complex, transsynaptic questions. When multiple binary expression systems are needed to label and manipulate different neuronal populations, as with pre- and postsynaptic neurons (Mosca and Luo 2014; Parisi et al. 2023), the required experiments must be carefully designed with limits on the ensuing number of transgenes (since multiple genetic drivers now contribute to the genetic load). In this case, 1 expression system would drive the expression of synaptic labels in 1 neuronal population while another expression system would drive an effector transgene in a second neuronal population. Employing a construct such as SynLight, which codes for multiple proteins from a single sequence, reduces the genetic load on the system and makes it easier to produce the correct experimental fly stocks in the absence of genetic dilution. Additionally, this transgene can be recombined with other transgenes, further simplifying the creation of a desired stock. Finally, our use of SynLight presents further proof-of-principle of the utility of 2A peptides in vivo in *Drosophila*. Prior work established transgenes containing a Ca²⁺ reporter like GCaMP and a membrane label (Daniels et al. 2014). The use of T2A to produce

GAL4-expressing constructs at the end of a protein reporter or endogenous protein has also greatly enhanced neuronal circuit study (Diao and White 2012; Lee et al. 2018; Kondo et al. 2020). By including 2 different reporters for membranes and active zones, this greatly increases the number and kinds of experiments possible. Future versions can pair effectors and labels (like Brp-Short-mStraw and an activity-altering construct) or even enzymes and labels (like a FLPase and Brp-Short-mStraw) as needed to design different kinds of experiments. Overall, SynLight enables the high-resolution visualization of presynaptic active zones as well as neuronal membranes in vivo via a single transgene, thus reducing the genetic load on the system. We anticipate that this new approach will be applied throughout the central and peripheral nervous system to answer more complicated questions about circuit biology, neurodevelopment, and synaptic organization.

Data availability

All fly lines have been deposited with the Bloomington *Drosophila* Stock Center and are also available upon request. The final plasmids for all variants of SynLight have been deposited with the *Drosophila* Genetics Resource Center. The final construct sequence for SynLight is included in the online [Supplementary material](#).

[Supplemental material](#) available at G3 online.

Acknowledgments

We would like to thank all members of the Mosca Lab for their constant support, input, and critical discussion of the project. We would like to thank Dr. Kristen Davis, Alison DePew, and S. Zosimus for comments on the manuscript. We thank the Developmental Studies Hybridoma Bank (created by the NICHD of the NIH and maintained at The University of Iowa, Department of Biology, Iowa City, IA 52242, USA) for antibodies. Stocks obtained from the Bloomington *Drosophila* Stock Center (NIH P40OD018537) were used in this study, and we thank them for their service to the community. We thank the *Drosophila* Genetics Resource Center (NIH 2P40OD010949) for archiving our plasmids as well as FlyBase (NIH U41HG000739, S454486; NSF DBI-2035515, 2039324) for its service to the fly community.

Funding

This work was supported by the National Institutes of Health grants R00-DC013059 and R01-NS110907 and the Commonwealth of Pennsylvania (CURE) program of the Pennsylvania Department of Health grant 4100077067 (to TJM). Work in the TJM Lab is supported by grants from the Alfred P. Sloan Foundation, the Whitehall Foundation, the Thomas Jefferson University Synaptic Biology Center, and the Thomas Jefferson University Dean's Transformational Science Award.

Conflicts of interest

The author(s) declare no conflict of interest.

Author contributions

MAA and TJM designed the project; MAA, JH, MJP, and JCD performed the experiments; MAA, MJP, and JCD produced reagents; MAA and JH analyzed the data; and MAA, JH, MJP, JCD, and TJM wrote and edited the manuscript.

Literature cited

- Aimino MA, DePew AT, Restrepo L, Mosca TJ. 2023. Synaptic development in diverse olfactory neuron classes uses distinct temporal and activity-related programs. *J Neurosci.* 43(1):28–55. doi:10.1523/JNEUROSCI.0884-22.2022.
- Andlauer TFM, Scholz-Kornehl S, Tian R, Kirchner M, Babikir HA, Depner H, Loll B, Quentin C, Gupta VK, Holt MG, et al. 2014. Drep-2 is a novel synaptic protein important for learning and memory. *eLife.* 3:e03895. doi:10.7554/eLife.03895.
- Araki T, Osaka J, Kato Y, Shimozone M, Kawamura H, Iwanaga R, Hakeda-Suzuki S, Suzuki T. 2020. Systematic identification of genes regulating synaptic remodeling in the *Drosophila* visual system. *Genes Genet Syst.* 95(3):101–110. doi:10.1266/ggs.19-00066.
- Bennett MR. 2011. Schizophrenia: susceptibility genes, dendritic-spine pathology and gray matter loss. *Prog Neurobiol.* 95(3):275–300. doi:10.1016/j.pneurobio.2011.08.003.
- Berger-Müller S, Sugie A, Takahashi F, Tavosanis G, Hakeda-Suzuki S, Suzuki T. 2013. Assessing the role of cell-surface molecules in central synaptogenesis in the *Drosophila* visual system. *PLoS One.* 8(12):e83732. doi:10.1371/journal.pone.0083732.
- Bolte S, Cordelières FP. 2006. A guided tour into subcellular colocalization analysis in light microscopy. *J Microsc.* 224(3):213–232. doi:10.1111/j.1365-2818.2006.01706.x.
- Bonasco C, Fuenzalida M. 2016. Plasticity of hippocampal excitatory-inhibitory balance: missing the synaptic control in the epileptic brain. *Neural Plast.* 2016:8607038. doi:10.1155/2016/8607038.
- Brand AH, Perrimon N. 1993. Targeted gene expression as a means of altering cell fates and generating dominant phenotypes. *Development.* 118(2):401–415. doi:10.1242/dev.118.2.401.
- Carrillo RA, Özkan E, Menon KP, Nagarkar-Jaiswal S, Lee PT, Jeon M, Birnbaum ME, Bellen HJ, Garcia KC, Zinn K. 2015. Control of synaptic connectivity by a network of *Drosophila* IgSF cell surface proteins. *Cell.* 163(7):1770–1782. doi:10.1016/j.cell.2015.11.022.
- Certel SJ, McCabe BD, Stowers RS. 2022. A conditional GABAergic synaptic vesicle marker for *Drosophila*. *J Neurosci Methods.* 372:109540. doi:10.1016/j.jneumeth.2022.109540.
- Certel SJ, Ruchti E, McCabe BD, Stowers RS. 2022. A conditional glutamatergic synaptic vesicle marker for *Drosophila*. *G3 (Bethesda).* 12(3):jkab453. doi:10.1093/g3journal/jkab453.
- Chen Y, Akin O, Nern A, Tsui CYK, Pecot MY, Zipursky SL. 2014. Cell-type-specific labeling of synapses in vivo through synaptic tagging with recombination. *Neuron.* 81(2):280–293. doi:10.1016/j.neuron.2013.12.021.
- Choi BJ, Chen YCD, Desplan C. 2021. Building a circuit through correlated spontaneous neuronal activity in the developing vertebrate and invertebrate visual systems. *Genes Dev.* 35(9–10):677–691. doi:10.1101/GAD.348241.121.
- Chou VT, Johnson SA, Van Vactor D. 2020. Synapse development and maturation at the *Drosophila* neuromuscular junction. *Neural Dev.* 15(1):11. doi:10.1186/s13064-020-00147-5.
- Chou YH, Spletter ML, Yaksi E, Leong JCS, Wilson RI, Luo L. 2010. Diversity and wiring variability of olfactory local interneurons in the *Drosophila* antennal lobe. *Nat Neurosci.* 13(4):439–449. doi:10.1038/nn.2489.
- Christiansen F, Zube C, Andlauer TFM, Wichmann C, Fouquet W, Oswald D, Mertel S, Leiss F, Tavosanis G, Luna AJF, et al. 2011. Presynapses in Kenyon cell dendrites in the mushroom body calyx of *Drosophila*. *J Neurosci.* 31(26):9696–9707. doi:10.1523/JNEUROSCI.6542-10.2011.
- Clandinin TR, Zipursky SL. 2002. Making connections in the fly visual system. *Neuron.* 35(5):827–841. doi:10.1016/S0896-6273(02)00876-0.
- Coates KE, Calle-Schuler SA, Helmick LM, Knotts VL, Martik BN, Salman F, Warner LT, Valla SV, Bock DD, Dacks AM. 2020. The wiring logic of an identified serotonergic neuron that spans sensory networks. *J Neurosci.* 40(33):6309–6327. doi:10.1523/JNEUROSCI.055220.2020.
- Coates KE, Majot AT, Zhang X, Michael CT, Spitzer SL, Gaudry Q, Dacks AM. 2017. Identified serotonergic modulatory neurons have heterogeneous synaptic connectivity within the olfactory system of *Drosophila*. *J Neurosci.* 37(31):7318–7331. doi:10.1523/JNEUROSCI.0192-17.2017.
- Collins CA, DiAntonio A. 2007. Synaptic development: insights from *Drosophila*. *Curr Opin Neurobiol.* 17(1):35–42. doi:10.1016/j.comb.2007.01.001.
- Daniels RW, Gelfand MV, Collins CA, DiAntonio A. 2008. Visualizing glutamatergic cell bodies and synapses in *Drosophila* larval and adult CNS. *J Comparative Neurol.* 508(1):131–152. doi:10.1002/cne.21670.
- Daniels RW, Rossano AJ, Macleod GT, Ganetzky B. 2014. Expression of multiple transgenes from a single construct using viral 2A peptides in *Drosophila*. *PLoS One.* 9(6):e100637. doi:10.1371/journal.pone.0100637.
- de Ramon Francàs G, Zuñiga NR, Stoeckli ET. 2017. The spinal cord shows the way—how axons navigate intermediate targets. *Dev Biol.* 432(1):43–52. doi:10.1016/j.ydbio.2016.12.002.
- Diao F, White BH. 2012. A novel approach for directing transgene expression in *Drosophila*: T2A-Gal4 in-frame fusion. *Genetics.* 190(3):1139–1144. doi:10.1534/genetics.111.136291.
- Dietzl G, Chen D, Schnorrrer F, Su KC, Barinova Y, Fellner M, Gasser B, Kinsey K, Oettel S, Scheiblaue S, et al. 2007. A genome-wide transgenic RNAi library for conditional gene inactivation in *Drosophila*. *Nature.* 448(7150):151–156. doi:10.1038/nature05954.
- Douin V, Bornes S, Creancier L, Rochaix P, Favre G, Prats AC, Couderc B. 2004. Use and comparison of different internal ribosomal entry sites (IRES) in tricistronic retroviral vectors. *BMC Biotechnol.* 4(1):16. doi:10.1186/1472-6750-4-16.
- Duhart JC, Mosca TJ. 2022. Genetic regulation of central synapse formation and organization in *Drosophila melanogaster*. *Genetics.* 221(3):iyac078. doi:10.1093/genetics/iyac078.
- Ehmann N, Oswald D, Kittel RJ. 2018. *Drosophila* active zones: from molecules to behaviour. *Neurosci Res.* 127:14–24. doi:10.1016/j.neures.2017.11.015.
- Estes PS, Ho GLY, Narayanan R, Ramaswami M. 2000. Synaptic localization and restricted diffusion of a *Drosophila* neuronal synaptobrevin—green fluorescent protein chimera in vivo. *J Neurogenet.* 13(4):233–255. doi:10.3109/01677060009084496.
- Farhy-Tselnicker I, Allen NJ. 2018. Astrocytes, neurons, synapses: a tripartite view on cortical circuit development. *Neural Dev.* 13(1):7. doi:10.1186/s13064-018-0104-y.
- Fendl S, Vieira RM, Borst A. 2020. Conditional protein tagging methods reveal highly specific subcellular distribution of ion channels in motion-sensing neurons. *eLife.* 9:e62953. doi:10.7554/eLife.62953.
- Fouquet W, Oswald D, Wichmann C, Mertel S, Depner H, Dyba M, Hallermann S, Kittel RJ, Eimer S, Sigrist SJ. 2009. Maturation of active zone assembly by *Drosophila bruchpilot*. *J Cell Biol.* 186(1):129–145. doi:10.1083/jcb.200812150.
- Fulterer A, Andlauer TFM, Ender A, Maglione M, Eyring K, Woitkuhn J, Lehmann M, Matkovic-Rachid T, Geiger JRP, Walter AM, et al. 2018. Active zone scaffold protein ratios tune functional diversity across brain synapses. *Cell Rep.* 23(5):1259–1274. doi:10.1016/j.celrep.2018.03.126.
- González M, Martín-Ruiz I, Jiménez S, Pirone L, Barrio R, Sutherland JD. 2011. Generation of stable *Drosophila* cell lines using multicistronic vectors. *Sci Rep.* 1:75. doi:10.1038/srep00075.

- Grabe V, Sachse S. 2018. Fundamental principles of the olfactory code. *BioSystems*. 164:94–101. doi:[10.1016/j.biosystems.2017.10.010](https://doi.org/10.1016/j.biosystems.2017.10.010).
- Grant SGN. 2012. Synaptopathies: diseases of the synaptome. *Curr Opin Neurobiol*. 22(3):522–529. doi:[10.1016/j.conb.2012.02.002](https://doi.org/10.1016/j.conb.2012.02.002).
- Grieger JC, Samulski RJ. 2005. Packaging capacity of adeno-associated virus serotypes: impact of larger genomes on infectivity and postentry steps. *J Virol*. 79(15):9933–9944. doi:[10.1128/jvi.79.15.9933-9944.2005](https://doi.org/10.1128/jvi.79.15.9933-9944.2005).
- Groth AC, Fish M, Nusse R, Calos MP. 2004. Construction of transgenic *Drosophila* by using the site-specific integrase from phage ϕ C31. www.fruitfly.org/blast/index.html
- Hallam EA, Carlson JR. 2006. Coding of odors by a receptor repertoire. *Cell*. 125(1):143–160. doi:[10.1016/j.cell.2006.01.050](https://doi.org/10.1016/j.cell.2006.01.050).
- Hasegawa K, Cowan AB, Nakatsuji N, Suemori H. 2007. Efficient multicistronic expression of a transgene in human embryonic stem cells. *Stem Cells*. 25(7):1707–1712. doi:[10.1634/stemcells.2006-0813](https://doi.org/10.1634/stemcells.2006-0813).
- Hummel T, Zipursky SL. 2004. Afferent induction of olfactory glomeruli requires N-cadherin. *Neuron*. 42(1):77–88. doi:[10.1016/S0896-6273\(04\)00158-8](https://doi.org/10.1016/S0896-6273(04)00158-8).
- Jan LY, Jan YN. 1982. Antibodies to horseradish peroxidase as specific neuronal markers in *Drosophila* and in grasshopper embryos. *Proc Natl Acad Sci U S A*. 79(8):2700–2704. doi:[10.1073/pnas.79.8.2700](https://doi.org/10.1073/pnas.79.8.2700).
- Jefferis GSXE, Marin EC, Stocker RF, Luo L. 2001. Target neuron pre-specification in the olfactory map of *Drosophila*. *Nature*. 414(6860):204–208. doi:[10.1038/35102574](https://doi.org/10.1038/35102574).
- Jefferis GSXE, Potter CJ, Chan AM, Marin EC, Rohlffing T, Maurer CR, Luo L. 2007. Comprehensive maps of *Drosophila* higher olfactory centers: spatially segregated fruit and pheromone representation. *Cell*. 128(6):1187–1203. doi:[10.1016/j.cell.2007.01.040](https://doi.org/10.1016/j.cell.2007.01.040).
- Jefferis GSXE, Vyas RM, Berdnik D, Ramaekers A, Stocker RF, Tanaka NK, Ito K, Luo L. 2003. Developmental origin of wiring specificity in the olfactory system of *Drosophila*. *Development*. 131(1):117–130. doi:[10.1242/dev.00896](https://doi.org/10.1242/dev.00896).
- Jenett A, Rubin GM, Ngo TTB, Shepherd D, Murphy C, Dionne H, Pfeiffer BD, Cavallaro A, Hall D, Jeter J, et al. 2012. A GAL4-driver line resource for *Drosophila* neurobiology. *Cell Rep*. 2(4):991–1001. doi:[10.1016/j.celrep.2012.09.011](https://doi.org/10.1016/j.celrep.2012.09.011).
- Karuppudurai T, Lin TY, Ting CY, Pursley R, Melnattur KV, Diao F, White BH, Macpherson LJ, Gallio M, Pohida T, et al. 2014. A hard-wired glutamatergic circuit pools and relays UV signals to mediate spectral preference in *Drosophila*. *Neuron*. 81(3):603–615. doi:[10.1016/j.neuron.2013.12.010](https://doi.org/10.1016/j.neuron.2013.12.010).
- Kaufman RJ, Davies MV, Wasley LC, Michnick D. 1991. Improved vectors for stable expression of foreign genes in mammalian cells by use of the untranslated leader sequence from EMC virus. *Nucleic Acids Res*. 19(16):4485–4490. doi:[10.1093/nar/19.16.4485](https://doi.org/10.1093/nar/19.16.4485).
- Kawamura H, Hakeda-Suzuki S, Suzuki T. 2020. Activity-dependent endocytosis of wingless regulates synaptic plasticity in the *Drosophila* visual system. *Genes Genet Syst*. 95(5):235–247. doi:[10.1266/ggs.20-00030](https://doi.org/10.1266/ggs.20-00030).
- Kim JH, Lee SR, Li LH, Park HJ, Park JH, Lee KY, Kim MK, Shin BA, Choi SY. 2011. High cleavage efficiency of a 2A peptide derived from porcine teschovirus-1 in human cell lines, zebrafish and mice. *PLoS One*. 6(4):e18556. doi:[10.1371/journal.pone.0018556](https://doi.org/10.1371/journal.pone.0018556).
- Kittel RJ, Wichmann C, Rasse TM, Fouquet W, Schmidt M, Schmid A, Wagh DA, Pawlu C, Kellner RR, Willig KI, et al. 2006. Bruchpilot promotes active zone assembly, Ca^{2+} channel clustering, and vesicle release. *Science*. 312(5776):1051–1054. doi:[10.1126/science.1126308](https://doi.org/10.1126/science.1126308).
- Kondo S, Takahashi T, Yamagata N, Imanishi Y, Katow H, Hiramatsu S, Lynn K, Abe A, Kumaraswamy A, Tanimoto H. 2020. Neurochemical organization of the *Drosophila* brain visualized by endogenously tagged neurotransmitter receptors. *Cell Rep*. 30(1):284–297.e5. doi:[10.1016/j.celrep.2019.12.018](https://doi.org/10.1016/j.celrep.2019.12.018).
- Krantz DE, Zipursky SL. 1990. *Drosophila* Chaoptin, a member of the leucine-rich repeat family, is a photoreceptor cell-specific adhesion molecule. *EMBO J*. 9(6):1969–1977. doi:[10.1002/j.1460-2075.1990.tb08325.x](https://doi.org/10.1002/j.1460-2075.1990.tb08325.x).
- Kremer MC, Christiansen F, Leiss F, Paehler M, Knapke S, Andlauer TFM, Förstner F, Kloppenburg P, Sigrist SJ, Tavosanis G. 2010. Structural long-term changes at mushroom body input synapses. *Curr Biol*. 20(21):1938–1944. doi:[10.1016/j.cub.2010.09.060](https://doi.org/10.1016/j.cub.2010.09.060).
- Laissue PP, Reiter C, Hiesinger PR, Halter S, Fischbach KF, Stocker RF. 1999. Three-dimensional reconstruction of the antennal lobe in. *J Comp Neurol*. 405(4):543–552. doi:[10.1002/\(SICI\)1096-9861\(19990322\)405:4<543::AID-CNE7>3.0.CO;2-A](https://doi.org/10.1002/(SICI)1096-9861(19990322)405:4<543::AID-CNE7>3.0.CO;2-A).
- Landgraf M, Thor S. 2006. Development of *Drosophila* motoneurons: specification and morphology. *Semin Cell Dev Biol*. 17(1):3–11. doi:[10.1016/j.semcdb.2005.11.007](https://doi.org/10.1016/j.semcdb.2005.11.007).
- Le T, Yu M, Williams B, Goel S, Paul SM, Beitel GJ. 2007. Casper5, a family of *Drosophila* transgenesis and shuttle vectors with improved multiple cloning sites. *Bone*. 42(3):164–166. doi:[10.2144/000112386](https://doi.org/10.2144/000112386).
- Lee T, Lee A, Luo L. 1999. Development of the *Drosophila* mushroom bodies: sequential generation of three distinct types of neurons from a neuroblast. *Development*. 126(18):4065–4076. doi:[10.1242/dev.126.18.4065](https://doi.org/10.1242/dev.126.18.4065).
- Lee T, Luo L. 1999. Mosaic analysis with a repressible neurotechnique cell marker for studies of gene function in neuronal morphogenesis. *Neuron*. 22(3):451–461. doi:[10.1016/S0896-6273\(00\)80701-1](https://doi.org/10.1016/S0896-6273(00)80701-1).
- Lee PT, Zirin J, Kanca O, Lin WW, Schulze KL, Li-Kroeger D, Tao R, Devereaux C, Hu Y, Chung V, et al. 2018. A gene-specific T2A-GAL4 library for *Drosophila*. *eLife*. 7:e35574. doi:[10.7554/eLife.35574](https://doi.org/10.7554/eLife.35574).
- Leisegang M, Engels B, Meyerhuber P, Kieback E, Sommermeyer D, Xue SA, Reuß S, Stauss H, Uckert W. 2008. Enhanced functionality of T cell receptor-redirection T cells is defined by the transgene cassette. *J Mol Med*. 86(5):573–583. doi:[10.1007/s00109-008-0317-3](https://doi.org/10.1007/s00109-008-0317-3).
- Leiss F, Groh C, Butcher NJ, Meinertzhagen IA, Tavosanis G. 2009. Synaptic organization in the adult *Drosophila* mushroom body calyx. *J Comp Neurol*. 517(6):808–824. doi:[10.1002/cne.22184](https://doi.org/10.1002/cne.22184).
- Leiss F, Koper E, Hein I, Fouquet W, Lindner J, Sigrist S, Tavosanis G. 2009. Characterization of dendritic spines in the *Drosophila* central nervous system. *Dev Neurobiol*. 69(4):221–234. doi:[10.1002/dneu.20699](https://doi.org/10.1002/dneu.20699).
- Liang L, Li Y, Potter CJ, Yizhar O, Deisseroth K, Tsien RW, Luo L. 2013. GABAergic projection neurons route selective olfactory inputs to specific higher-order neurons. *Neuron*. 79(5):917–931. doi:[10.1016/j.neuron.2013.06.014](https://doi.org/10.1016/j.neuron.2013.06.014).
- Lin DM, Goodman CS. 1994. Ectopic and increased expression of fasciclin II alters motoneuron growth cone guidance. *Neuron*. 13(3):507–523. doi:[10.1016/0896-6273\(94\)90022-1](https://doi.org/10.1016/0896-6273(94)90022-1).
- Liu KS, Siebert M, Mertel S, Knoche E, Wegener S, Wichmann C, Matkovic T, Muhammad K, Davis GW, Schmitz D, et al. 2011. RIM-binding protein, a central part of the active zone, is essential for neurotransmitter release. *Science*. 334(6062):1565–1569. doi:[10.1126/science.1212991](https://doi.org/10.1126/science.1212991).
- Luke GA, Escuin H, De Felipe P, Ryan MD. 2009. 2A to the fore—research, technology and applications. *Biotechnol Genet Eng Rev*. 26(1):223–260. doi:[10.5661/bger-26-223](https://doi.org/10.5661/bger-26-223).
- Manders EMM, Verbeek FJ, Aten JA. 1993. Measurement of colocalization of objects in dual-colour confocal images. *J Microsc*. 169(3):375–382. doi:[10.1111/j.1365-2818.1993.tb03313.x](https://doi.org/10.1111/j.1365-2818.1993.tb03313.x).
- Martínez-Salas E. 1999. Internal ribosome entry site biology and its use in expression vectors. *Curr Opin Biotechnol*. 10(5):458–464. doi:[10.1016/S0958-1669\(99\)00010-5](https://doi.org/10.1016/S0958-1669(99)00010-5).
- Menon KP, Carrillo RA, Zinn K. 2013. Development and plasticity of the *Drosophila* larval neuromuscular junction. *Dev Biol*. 2(5):647–670. doi:[10.1002/wdev.108](https://doi.org/10.1002/wdev.108).

- Mizuguchi H, Xu Z, Ishii-Watabe A, Uchida E, Hayakawa T. 2000. IRES-dependent second gene expression is significantly lower than cap-dependent first gene expression in a bicistronic vector. *Mol Ther.* 1(4):376–382. doi:10.1006/mthe.2000.0050.
- Mosca TJ, Luginbuhl DJ, Wang IE, Luo L. 2017. Presynaptic LRP4 promotes synapse number and function of excitatory CNS neurons. *eLife.* 6:e27347. doi:10.7554/eLife.27347.
- Mosca TJ, Luo L. 2014. Synaptic organization of the *Drosophila* antennal lobe and its regulation by the teneurins. *eLife.* 3:e03726. doi:10.7554/eLife.03726.
- Mosca TJ, Schwarz TL. 2010. The nuclear import of frizzled2-C by importins- β 211 and $\hat{I} \pm 2$ promotes postsynaptic development. *Nat Neurosci.* 13(8):935–943. doi:10.1038/nn.2593.
- Mullins C, Fishell G, Tsien RW. 2016. Unifying views of autism spectrum disorders: a consideration of autoregulatory feedback loops. *Neuron.* 89(6):1131–1156. doi:10.1016/j.neuron.2016.02.017.
- Naso MF, Tomkowicz B, Perry WL, Strohl WR. 2017. Adeno-associated virus (AAV) as a vector for gene therapy. *BioDrugs.* 31(4):317–334. doi:10.1007/s40259-017-0234-5.
- Nicolaï LJJ, Ramaekers A, Raemaekers T, Drozdzecki A, Mauss AS, Yan J, Landgraf M, Annaert W, Hassan BA. 2010. Genetically encoded dendritic marker sheds light on neuronal connectivity in *Drosophila*. *Proc Natl Acad Sci U S A.* 107(47):20553–20558. doi:10.1073/pnas.1010198107.
- Ohtsuka T, Takao-Rikitsu E, Inoue E, Inoue M, Takeuchi M, Matsubara K, Deguchi-Tawarada M, Satoh K, Morimoto K, Nakanishi H, et al. 2002. CAST: a novel protein of the cytomatrix at the active zone of synapses that forms a ternary complex with RIM1 and Munc13-1. *J Cell Biol.* 158(3):577–590. doi:10.1083/jcb.200202083.
- Osaka J, Yasuda H, Watanuki Y, Kato Y, Nitta Y, Sugie A, Sato M, Suzuki T. 2023. Identification of genes regulating stimulus-dependent synaptic assembly in *Drosophila* using an automated synapse quantification system. *Genes Genetic Syst.* 97(6):297–309 doi:10.1266/ggs.22-00114.
- Özel MN, Kulkarni A, Hasan A, Brummer J, Moldenhauer M, Daumann IM, Wolfenberger H, Dercksen VJ, Kiral FR, Weiser M, et al. 2019. Serial synapse formation through filopodial competition for synaptic seeding factors. *Dev Cell.* 50(4):447–461.e8. doi:10.1016/j.devcel.2019.06.014.
- Parisi MJ, Aimino MA, Mosca TJ. 2023. A conditional strategy for cell-type-specific labeling of endogenous excitatory synapses in *Drosophila*. *Cell Rep Methods.* 3(5):100477. doi:10.1016/j.crmeth.2023.100477.
- Potter CJ, Tasic B, Russler EV, Liang L, Luo L. 2010. The Q system: a repressible binary system for transgene expression, lineage tracing, and mosaic analysis. *Cell.* 141(3):536–548. doi:10.1016/j.cell.2010.02.025.
- Restrepo LJ, DePew AT, Moese ER, Tymanskyj SR, Parisi MJ, Aimino MA, Duhart JC, Fei H, Mosca TJ. 2022. γ -secretase promotes *Drosophila* postsynaptic development through the cleavage of a Wnt receptor. *Dev Cell.* 57(13):1643–1660.e7. doi:10.1016/j.devcel.2022.05.006.
- Riabinina O, Luginbuhl D, Marr E, Liu S, Wu MN, Luo L, Potter CJ. 2015. Improved and expanded Q-system reagents for genetic manipulations. *Nat Methods.* 12(3):219–222. doi:10.1053/j.gastro.2016.08.014. CagY.
- Sánchez-Soriano N, Bottenberg W, Fiala A, Haessler U, Kerassoviti A, Knust E, Löhr R, Prokop A. 2005. Are dendrites in *Drosophila* homologous to vertebrate dendrites? *Dev Biol.* 288(1):126–138. doi:10.1016/j.ydbio.2005.09.026.
- Scheffer LK, Xu CS, Januszewski M, Lu Z, Takemura SY, Hayworth KJ, Huang GB, Shinomiya K, Maitin-Shepard J, Berg S, et al. 2020. A connectome and analysis of the adult *Drosophila* central brain. *eLife.* 9:e57443. doi:10.7554/ELIFE.57443.
- Shimozono M, Osaka J, Kato Y, Araki T, Kawamura H, Takechi H, Hakeda-Suzuki S, Suzuki T. 2019. Cell surface molecule, Klingon, mediates the refinement of synaptic specificity in the *Drosophila* visual system. *Genes Cells.* 24(7):496–510. doi:10.1111/gtc.12703.
- Siddiqui TJ, Craig AM. 2011. Synaptic organizing complexes. *Curr Opin Neurobiol.* 21(1):132–143. doi:10.1016/j.conb.2010.08.016.
- Silbereis JC, Pochareddy S, Zhu Y, Li M, Sestan N. 2016. The cellular and molecular landscapes of the developing human central nervous system. *Neuron.* 89(2):248. doi:10.1016/j.neuron.2015.12.008.
- Stockinger P, Kvitsiani D, Rotkopf S, Tirián L, Dickson BJ. 2005. Neural circuitry that governs *Drosophila* male courtship behavior. *Cell.* 121(5):795–807. doi:10.1016/j.cell.2005.04.026.
- Südhof TC. 2012. The presynaptic active zone. *Neuron.* 75(1):11–25. doi:10.1016/j.neuron.2012.06.012.
- Sugie A, Hakeda-Suzuki S, Suzuki E, Silies M, Shimozono M, Möhl C, Suzuki T, Tavosanis G. 2015. Molecular remodeling of the presynaptic active zone of *Drosophila* photoreceptors via activity-dependent feedback. *Neuron.* 86(3):711–725. doi:10.1016/j.neuron.2015.03.046.
- Suh GSB, Wong AM, Hergarden AC, Wang JW, Simon AF, Benzer S, Axel R, Anderson DJ. 2004. A single population of olfactory sensory neurons mediates an innate avoidance behaviour in *Drosophila*. *Nature.* 431(7010):854–859. doi:10.1038/nature02980.
- Takemura SY, Bharioke A, Lu Z, Nern A, Vitaladevuni S, Rivlin PK, Katz WT, Olbris DJ, Plaza SM, Winston P, et al. 2013. A visual motion detection circuit suggested by *Drosophila* connectomics. *Nature.* 500(7461):175–181. doi:10.1038/nature12450.
- Takemura SY, Xu CS, Lu Z, Rivlin PK, Parag T, Olbris DJ, Plaza S, Zhao T, Katz WT, Umayam L, et al. 2015. Synaptic circuits and their variations within different columns in the visual system of *Drosophila*. *Proc Natl Acad Sci U S A.* 112(44):13711–13716. doi:10.1073/pnas.1509820112.
- Tanaka NK, Ito K, Stopfer M. 2009. Odor-evoked neural oscillations in *Drosophila* are mediated by widely branching interneurons. *J Neurosci.* 29(26):8595–8603. doi:10.1523/jneurosci.1455-09.2009.
- Tang W, Ehrlich I, Wolff SBE, Michalski AM, Wöfl S, Hasan MT, Lüthi A, Sprengel R. 2009. Faithful expression of multiple proteins via 2A-peptide self-processing: a versatile and reliable method for manipulating brain circuits. *J Neurosci.* 29(27):8621–8629. doi:10.1523/JNEUROSCI.0359-09.2009.
- Underhill MF, Smales CM, Naylor LH, Birch JR, James DC. 2007. Transient gene expression levels from multigene expression vectors. *Biotechnol Prog.* 23(2):435–443. doi:10.1021/bp060225z.
- Venken KJT, He Y, Hoskins RA, Bellen HJ. 2006. P[acman]: A BAC transgenic platform for targeted insertion of large DNA fragments in *D. melanogaster*. <https://www.science.org>
- Venken KJT, Schulze KL, Haelterman NA, Pan H, He Y, Evans-Holm M, Carlson JW, Levis RW, Spradling AC, Hoskins RA, et al. 2011. MiMIC: a highly versatile transposon insertion resource for engineering *Drosophila melanogaster* genes. *Nat Methods.* 8(9):737–743. doi:10.1038/nmeth.1662.
- Venken KJT, Simpson JH, Bellen HJ. 2011. Genetic manipulation of genes and cells in the nervous system of the fruit fly. *Neuron.* 72(2):202–230. doi:10.1016/j.neuron.2011.09.021.
- Vosshall LB, Wong AM, Axel R. 2000. An olfactory sensory map in the fly brain. *Cell.* 102(2):147–159. doi:10.1016/s0092-8674(00)00021-0.
- Wagh DA, Rasse TM, Asan E, Hofbauer A, Schwenkert I, Dürrbeck H, Buchner S, Dabauvalle MC, Schmidt M, Qin G, et al. 2006. Bruchpilot, a protein with homology to ELKS/CAST, is required for structural integrity and function of synaptic active zones in *Drosophila*. *Neuron.* 49(6):833–844. doi:10.1016/j.neuron.2006.02.008.
- Wairkar YP, Fradkin LG, Noordermeer JN, DiAntonio A. 2008. Synaptic defects in a *Drosophila* model of congenital muscular dystrophy. *J*

- Neurosci. 28(14):3781–3789. doi:[10.1523/JNEUROSCI.0478-08.2008](https://doi.org/10.1523/JNEUROSCI.0478-08.2008).
- Waites CL, Craig AM, Garner CC. 2005. Mechanisms of vertebrate synaptogenesis. *Ann Rev Neurosci.* 28(1):251–274. doi:[10.1146/annurev.neuro.27.070203.144336](https://doi.org/10.1146/annurev.neuro.27.070203.144336).
- Wang Y, Liu X, Biederer T, Sü TC. 2002. A family of RIM-binding proteins regulated by alternative splicing: implications for the genesis of synaptic active zones. *Proc Natl Acad Sci U S A.* 29(22):14464–14469. doi:[10.1073/pnas.182532999](https://doi.org/10.1073/pnas.182532999).
- Weinholtz CA, Castle MJ. 2021. Intersectional targeting of defined neural circuits by adeno-associated virus vectors. *J Neurosci Res.* 99(4):981–990. doi:[10.1002/jnr.24774](https://doi.org/10.1002/jnr.24774).
- Williams JL, Shearin HK, Stowers RS. 2019. Conditional synaptic vesicle markers for *Drosophila*. *G3 (Bethesda).* 9(3):737–748. doi:[10.1534/g3.118.200975](https://doi.org/10.1534/g3.118.200975).
- Wilson RI. 2013. Early olfactory processing in *Drosophila*: mechanisms and principles. *Ann Rev Neurosci.* 36(1):217–241. doi:[10.1146/annurev-neuro-062111-150533](https://doi.org/10.1146/annurev-neuro-062111-150533).
- Wu JS, Luo L. 2006. A protocol for dissecting *Drosophila melanogaster* brains for live imaging or immunostaining. *Nat Protocols.* 1(4):2110–2115. doi:[10.1038/nprot.2006.336](https://doi.org/10.1038/nprot.2006.336).
- Wu Z, Yang H, Colosi P. 2010. Effect of genome size on AAV vector packaging. *Mol Therapy.* 18(1):80–86. doi:[10.1038/mt.2009.255](https://doi.org/10.1038/mt.2009.255).
- Yang HH, Clandinin TR. 2018. Elementary motion detection in *Drosophila*: algorithms and mechanisms. *Annu Rev Vis.* 15(4):139–143–163. doi:[10.1146/annurev-vision-091517-034153.Elementary](https://doi.org/10.1146/annurev-vision-091517-034153.Elementary).
- Ye X, Fong P, Iizuka N, Choate D, Cavener DR. 1997. Ultrabithorax and antennapedia 5 untranslated regions promote developmentally regulated internal translation initiation. *Mol Cell Biol.* 17(3):1714–1721. doi:[10.1128/MCB.17.3.1714](https://doi.org/10.1128/MCB.17.3.1714).
- Zhang YQ, Rodesch CK, Broadie K. 2002. Living synaptic vesicle marker: synaptotagmin-GFP. *Genesis.* 34(1–2):142–145. doi:[10.1002/gene.10144](https://doi.org/10.1002/gene.10144).

Editor: J. Tennesen